

A Survey on All-in-One Image Restoration: Taxonomy, Evaluation and Future Trends

Junjun Jiang[✉], *Senior Member, IEEE*, Zengyuan Zuo, Gang Wu, Kui Jiang, and Xianming Liu, *Member, IEEE*

Abstract—Image restoration (IR) aims to recover high-quality images from inputs degraded by various factors such as noise, blur, compression, and adverse weather. Traditional IR methods typically focus on specific types of degradation, which limits their effectiveness in real-world scenarios with complex distortions. In response to this challenge, the all-in-one image restoration (AiOIR) paradigm has recently emerged, offering a unified framework that adeptly addresses multiple degradation types. These innovative models enhance convenience and versatility by adaptively learning degradation-specific features while simultaneously leveraging shared knowledge across diverse corruptions. In this survey, we present the first comprehensive overview of AiOIR, offering a taxonomy that organizes existing methods by architecture innovations, learning strategies, and key improvements. We systematically categorize prevailing approaches and critically assess the challenges these models encounter, proposing future research directions to propel this rapidly evolving field. Our survey begins with an introduction to the foundational concepts of AiOIR models, followed by a categorization of typical scenarios. We then highlight key architectural and algorithmic advances in AiOIR, aiming to inspire continued innovation. To facilitate rigorous evaluation of existing methods, we collate and summarize established datasets, evaluation metrics, and common experimental settings. Finally, we present an objective comparison of open-sourced methods, providing valuable insights for researchers and practitioners. This paper stands as the first comprehensive and insightful review of all-in-one image restoration. A related repository is available at <https://github.com/Harbinzzy/All-in-One-Image-Restoration-Survey>.

Index Terms—All-in-One Model, Image Restoration, Computer Vision, Deep Learning

I. INTRODUCTION

IMAGE processing is an integral part of low-level vision tasks, and digital image processing has evolved significantly over the past few decades, transitioning from traditional methods to advanced deep learning techniques. These methods, while effective, are limited by their inability to handle complex and varied image degradation scenarios. With the rise of deep learning, image processing has achieved remarkable results, especially driven by convolutional neural networks (CNNs) [1], Transformers [2]. In the image restoration (IR) field, single-task IR has achieved notable breakthroughs in correcting a specific type of image degradation (e.g., denoising [3]–[8], dehazing [9]–[13], desnowing [14]–[16], deraining [17]–[19], deblurring [20], [21] and low-light image

J. Jiang, Z. Zuo, G. Wu, K. Jiang, and X. Liu are with the School of Computer Science and Technology, Harbin Institute of Technology, Harbin 150001, China.

enhancement [22]–[24]). Although they have set state-of-the-art performance on restoring diverse degraded images, existing single-task IR methods generally lack the flexibility to adapt to new types of image degradation without extensive retraining (it is worth noting that some real-world IR methods [25]–[28] are not categorized as single-task IR). To alleviate the aforementioned issues, researchers have proposed all-in-one image restoration (AiOIR), devoting significant effort to introduce various key improvements (e.g., prompt-based learning approach, mixture-of-experts structure, multimodal model and autonomous agent) beyond single-task IR.

The AiOIR approach aims to develop a model capable of addressing multiple isolated or mixed degradation tasks (e.g., denoising, deblurring, dehazing, deraining, and low-light enhancement) within a unified framework without the need for task-specific retraining. While single-task models often achieve state-of-the-art performance for specific restoration tasks, AiOIR models offer the potential for more efficient deployment and unified processing, particularly when handling unknown, mixed, or dynamically changing degradations. Despite the variety of AiOIR models, their ability to generate high-quality images is still under active exploration. Recently, pioneering researchers have been investigating ways to optimize the architectures of these models to balance the trade-offs between computational complexity and restoration quality.

With the rapid development of AiOIR, numerous researchers have collected a series of datasets tailored for various all-in-one task settings, e.g., the All-Weather dataset [29] for synthetic weather-related scenarios, the WeatherStream dataset [30] for real-world weather-related scenarios, the CDD-11 dataset [31] for composite degradations, etc. Leveraging these datasets, most recent works focus on improving the representation capability of IR networks for complicated degradation through well-designed methods based on prompt learning, contrastive learning, multimodal representations, etc. Although these works have achieved superior progress in the objective quality (e.g., PSNR, NIQE [32] and FID [33]), the restored images still suffer from unsatisfactory texture generation, hindering the application of IR methods in real-world scenarios. Collectively, these methodologies represent a substantial progression in the pursuit of sophisticated, accurate, and versatile AiOIR solutions.

AiOIR methods have emerged as a positive step forward, although their specific implementations and applications are still under exploration. While there are comprehensive surveys for single-task IR methods, such as image super-resolution [34]–[37], deraining [38], [39], dehazing [40], denoising [41]–[43], deblurring [44], [45], low-light enhancement [46]–[48], and

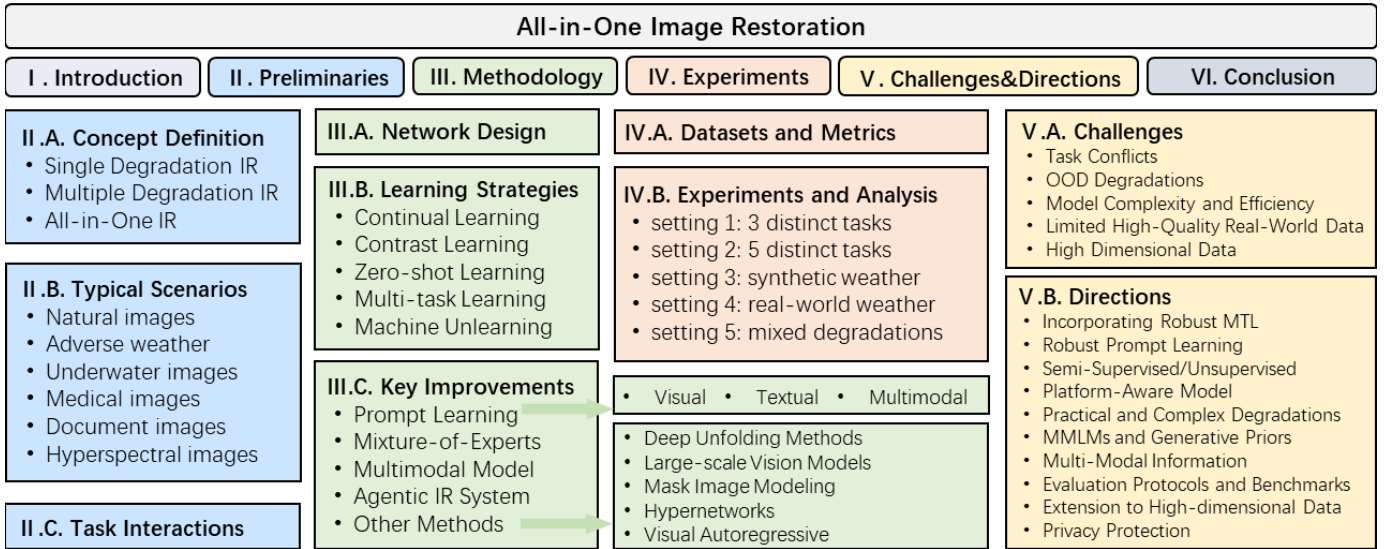


Fig. 1. Hierarchically-structured taxonomy of this survey.

the review covering diffusion-based image restoration [49], no existing review has systematically examined the emerging field of AiOIR. To bridge this gap, we aim to provide the first comprehensive overview of AiOIR methods, shedding light on both its representative approaches and diverse improvements. Fig. 1 shows the taxonomy of this survey in a hierarchically-structured way. In the following sections, we will cover various aspects of recent advances in AiOIR:

- 1) Preliminaries (Sec. II) : We introduce the definition of AiOIR and provide a comparison with related concepts. We point out typical scenarios and task relationships.
- 2) Methodology (Sec. III) : We provide a detailed analysis of representative AiOIR networks, aiming to illustrate the prevailing methods and elucidate the different categories of methods. By analyzing state-of-the-art methods, we summarize network architectures, learning strategies, and some key improvements.
- 3) Experiments (Sec. IV) : To facilitate a reasonable and exhaustive comparison, we clarify the commonly-used datasets and experimental settings in AiOIR. Furthermore, comprehensive comparisons across different settings are provided.
- 4) Challenges and Future Directions (Sec. V) : There are still some challenges to extending AiOIR to the practical applications. To further improve the development of AiOIR, we summarize the primary challenges and propose the potential directions and trends.

II. PRELIMINARIES

In this section, we first define the concept of all-in-one image restoration and compare it with related concepts. Subsequently, we provide a comprehensive review of diverse scenarios in AiOIR and the corresponding approaches. Finally, we illustrate the interactions between different IR tasks.

A. Concept Definitions

Single degradation image restoration (SDIR) focuses on recovering clean images from observations that have been corrupted by a specific type of degradation, such as noise [4]–[6], blur [20], [21], or rain [17]–[19]. These methods are typically task-specific, meaning that each model is designed for a particular degradation type. While these models demonstrate strong performance on known degradation types, they often exhibit limited generalization capability when encountering unseen degradation patterns or novel corruption intensities. Recently, some works [50]–[52] show certain generalizability to various degradation types with a unified framework. However, they need to train different models for different degradations, which are not all-in-one solutions as expected in practice. We refer to these methods as multiple degradation image restoration (MDIR). Subsequently, there have been recent attempts to unify multiple image restoration tasks within a single framework without the need for retraining. The seminal work [53] proposed the all-in-one weather restoration method which utilizes a multi-encoder and decoder architecture and the neural architecture search across task-specific optimized encoders. Moreover, Li *et al.* [54] first proposed the all-in-one blind image restoration using contrastive learning to extract degradation representations, which can recover images from multiple corruptions without any degradation information in advance. The AiOIR approach aims to recover clean images under various conditions explicitly tailored to address isolated or mixed degradation based on multi-head and multi-tail structures, priors, or pretrained models within a unified framework. It is worth noting that, some robust IR models [25]–[28], [55], [56] are still broadly considered part of the AiOIR setting. The AiOIR models present practical advantages such as reduced storage requirements and simplified deployment. However, the principal challenge lies in developing robust architectures capable of effectively addressing diverse degradations and achieving high-quality restorations across varying conditions in real-world scenarios.

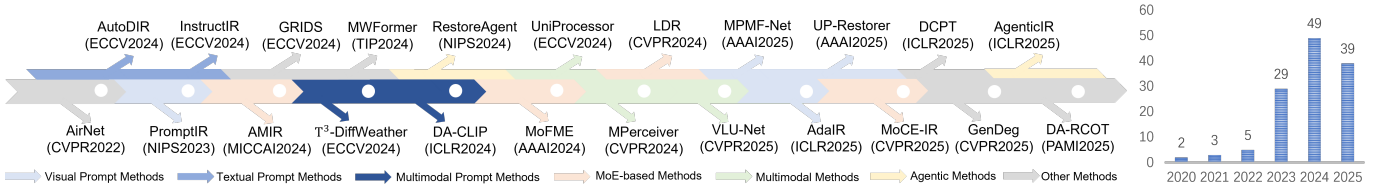


Fig. 2. Milestones of AiOIR methods. We simply list their names and venues. The bar chart shows the approximate annual number of papers on AiOIR from 2020 to May 2025.

B. Typical Scenarios

We categorize AiOIR into several scenarios according to types of images processed, including natural images, images under adverse weather conditions, underwater images, medical images, document images, and hyperspectral images.

Natural images. The degradation types commonly encountered in natural images include Gaussian noise, real-world noise, defocus blur, motion blur, low-light conditions, JPEG compression artifacts, mosaic effects, and issues arising from under-display cameras. Various AiOIR approaches have been developed to address these degradations, including techniques outlined in studies such as [57]–[62]. These approaches primarily focus on resolving typical problems found in both natural and man-made scenes, enhancing the quality and usability of images affected by these common degradations.

Adverse weather conditions. In more extreme cases, the images requiring restoration may be severely impacted by various adverse weather conditions, such as snowflakes, raindrops, and dense haze effects. These conditions lead to ill-posed inverse problems that are crucial for applications in autonomous navigation, video retrieval, and outdoor surveillance. The AiOIR field has seen the emergence of many solutions aiming at addressing these challenges, including works like [29], [63]–[67]. Notably, Liu *et al.* [68] proposed multi-weather nighttime image restoration. These solutions are designed to effectively restore visibility and clarity in images affected by harsh environmental conditions.

Underwater images. Underwater images suffer from wavelength-dependent light attenuation and scattering by marine microorganisms, leading to haze, color casts, low contrast, and loss of fine detail. UniUIR [56], a pioneering framework to tackle such compound distortions in an integrated manner, introduces the Mamba MoE module leveraging DepthAnythingV2 [69] to inject scene depth priors.

Medical images. The domain of medical imaging within AiOIR encompasses various types, including clinical computed tomography (CT), magnetic resonance imaging (MRI), and positron emission tomography (PET). Notable approaches in this area include AMIR [70] and ProCT [71]. AMIR utilizes a task-adaptive routing strategy that achieves state-of-the-art performance across three key medical imaging restoration tasks (*i.e.*, MRI super-resolution, CT denoising, and PET synthesis). Meanwhile, ProCT introduces an innovative view-aware prompting technique combined with artifact-aware contextual learning. This approach enables universal incomplete-view CT reconstruction and demonstrates seamless adaptability to out-of-domain hybrid CT scenarios.

Document images. DocRes [72] pioneers the exploration of generalist models for all-in-one restoration of document images. This work addresses five tasks (*i.e.*, dewarping, deshadowing, appearance enhancement, deblurring, and binarization). DocRes employs a straightforward yet highly effective visual prompting method known as DTSPrompt, which effectively distinguishes between different tasks and accommodates various resolutions. TextDoctor [73], utilizing the structure pyramid prediction and patch pyramid diffusion model, exhibits superior performance in capturing the structure of inpainted text.

Hyperspectral images. While effective for the RGB image restoration, all-in-one methods struggle with hyperspectral images (HSIs), as the complexity and variability of degradation hinder the generalization of common strategies. PromptHSI [74] integrates frequency-domain priors with the vision-language model driven prompt learning, and introduces a composite degradation dataset for all-in-one HSI restoration. MP-HSIR [75] further introduces a novel multi-prompt framework that integrates spectral, textual, and visual prompts. Unlike PromptHSI, MP-HSIR exploits complementary prompt modalities to better capture diverse degradation patterns and enhance spectral restoration.

C. Task Interactions

While the aforementioned taxonomy outlines various scenarios for AiOIR, problems in the real world are inherently complex. It remains crucial to understand the interactions between different restoration tasks, particularly in mixed-degradation scenarios, where multiple types of corruption co-occur (*e.g.*, low-light and blur). These task interactions can be complementary, independent, or even conflicting, significantly affecting the overall restoration quality and the design of unified models. For example:

- **Noise and blur:** High ISO or low-light settings often cause both sensor noise and motion blur. Noise may obscure blur kernels, while inaccurate deblurring can amplify noise residuals [76].
- **Rain, haze, and resolution:** In outdoor surveillance, rain streaks and haze not only degrade contrast but also interfere with spatial detail, complicating subsequent super-resolution.
- **Color and illumination distortions:** In underwater or adverse weather conditions, color shift, low contrast, and backscatter occur simultaneously, requiring integrated correction of color, visibility, and detail [77].

These intertwined degradations present both challenges (task entanglement, ordering sensitivity, domain ambiguity) and opportunities (shared features, multi-task learning, unified representations) for AiOIR models. Understanding these interdependencies is crucial for the design of robust and generalizable AiOIR systems, especially in unconstrained or real-world environments where degradation types and combinations are unpredictable.

III. METHODOLOGY

All-in-one image restoration methods have gained significant attention for their ability to address multiple types of degradation within a unified model. These methods are particularly valuable in real-world scenarios where images may be simultaneously affected by various artifacts, such as noise, blur, and adverse weather conditions. This section presents a comprehensive analysis of AiOIR methods from multiple perspectives. Firstly, we examine both novel and traditional network architectures, discussing their implementation approaches and classifying them into several typical network designs. Subsequently, we further investigate diverse learning strategies, which encompass training methodologies and perspectives, to improve image reconstruction accuracy and overall restoration quality. Finally, we examine other advanced techniques that optimize AiOIR models, including Prompt Learning, Mixture-of-Experts (MoE), Multimodal Model, and Agentic IR System. In Fig. 2, we present the representative works on AiOIR according to the timeline and method types.

A. Network Design for AiOIR

Existing all-in-one image restoration methods, as a form of multi-task learning (MTL), employ various architectural designs to handle inputs and outputs across multiple tasks, enabling efficient information sharing among them. Despite significant differences in their architectures, AiOIR methods can be broadly categorized into ten representative frameworks, as illustrated in Fig. 3 and described below.

(a) *Task-Specific Encoders and Decoders*: This straightforward approach assigns a specifically designed encoder-decoder pair to each type of degradation. For example, one encoder-decoder might handle low-light enhancement, while another addresses image denoising. This setup requires prior knowledge of the degradation type to select the appropriate components. However, in real-world scenarios, images often suffer from multiple or unknown degradations, making this approach less practical.

To overcome this limitation, models (b), (c), (d), and beyond aim to handle multiple degradation types within a unified framework without relying on prior knowledge, offering greater flexibility and efficiency.

(b) *Shared Decoder with Multiple Heads*: Models in this category share a common decoder but have multiple heads trained individually for different degradation types. For instance, Li *et al.* [53] proposed a method for processing various types of adverse weather images using shared weights, but requiring separate training for each degradation type.

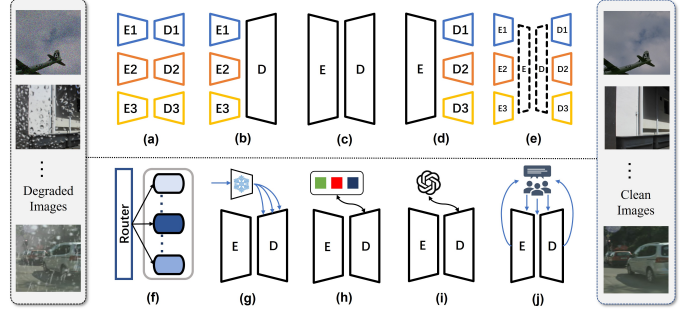


Fig. 3. Ten categories of the image restoration method prototype (the last nine are AiOIR methods) (a) independent encoders and decoders. (b) multiple heads and a shared decoder. (c) a single branch end-to-end model. (d) a shared encoder and multiple decoders. (e) a reusable pretrained middle-level backbone. (f) the mixture-of-experts architecture. (g) pretrained large vision-language models to guide image restoration. (h) visual prompts to guide image restoration. (i) textual prompts or instructions to guide image restoration. (j) a question answering paradigm.

(c) *Unified Encoder-Decoder Architecture*: These models use a single encoder-decoder architecture without separate heads or tails, often serving as foundational designs that can be adapted for multi-degradation removal. There are methods like TransWeather [29], AirNet [54], TANet [78], and AdaIR [79].

(d) *Shared Backbone with Multiple Decoders*: Universal models adopt mixed inputs without any task-specific indicators, using a shared backbone for feature extraction and multiple task-specific decoders. For example, BIDeN [80] follows this paradigm. However, this reintroduces the complexity of multiple decoders and requires extensive supervision with degradation labels.

(e) *Pretrained Mid-Level Backbone*: Some models introduce a reusable pretrained transformer backbone with task-specific heads and tails. IPT [81] leverages pretraining to address general noise removal, significantly simplifying the pipeline by utilizing prior knowledge.

(f) *Mixture-of-Experts Architecture*: In MoE-based models, inputs are routed to different experts via a gating mechanism. For instance, MEASNet [82] considers both pixel-level and global features (including low-frequency and high-frequency components) to select the appropriate expert for image restoration.

(g) *Pretrained Model Prior*: Models like DINO-IR [83], Perceive-IR [84], and DA-CLIP [85] utilize frozen vision-language models (e.g., CLIP [86], DINO [87], and DINO-v2 [88]). These models predict high-quality feature embeddings to enhance the restoration process by leveraging semantic alignment between vision and language.

(h) *Visual Prompting*: These models employ a single encoder-decoder architecture and inject learnable visual prompts at multiple decoding stages to implicitly predict degradation conditions. Examples include works like [58], [89]–[92]. The prompts guide the decoder in adaptively recovering various degraded images, serving as lightweight plug-and-play modules with minimal additional parameters.

(i) *Textual and Multimodal Prompting*: Extending the concept of prompting, models like [93]–[95] incorporate textual or multimodal prompts. These models allow for natural language

instructions or combine visual and textual cues to steer the restoration process, enhancing adaptability to unknown degradations.

(j) *Question-Answering Paradigm*: Finally, models such as PromptGIP [96] and AutoDIR [61] employ a question-answering framework. They empower users to customize image restoration according to their preferences by interpreting user inputs and adjusting the restoration process accordingly.

AiOIR models have evolved from task-specific architectures requiring prior knowledge of degradation types to more flexible and unified frameworks capable of handling multiple degradations without explicit information. Moreover, recent methods increasingly adopt hybrid designs, which we further categorize by their component labels. For example, (g+h) methods such as [97] combine DepthAnything [98] with learnable visual prompts; (f+h) methods like [82] use task-specific prompts to guide multi-expert selection; (f+i) methods like [99] leverage the power of pretrained vision-language models to enrich the diversity of weather-specific knowledge based on an MoE architecture; (h+i) methods, with representative works including [84], [100], embed both visual and textual prompts into a unified framework. With this concise labeling, emerging hybrids can be directly slotted into our taxonomy.

B. Learning Strategies of AiOIR

Besides network design (as discussed in Sec. III-A), robust learning strategies are crucial for achieving satisfactory results in AiOIR. In this section, we discuss several promising learning strategies in this field. We begin with continual learning, exploring how it can prevent catastrophic forgetting. Next, we focus on contrastive learning and its application in complex degradation scenarios, emphasizing its role in enhancing the discriminative power of image features. We then discuss the zero-shot learning in AiOIR, emphasizing its ability to generalize to unseen degradations. Additionally, we highlight the potential of multi-task learning (MTL) to optimize performance across various degradation tasks, pointing out the importance of addressing task relationships and conflicts. Finally, we introduce the concept of machine unlearning, exploring its potential for privacy protection.

1) *Continual Learning*: AiOIR methods can be categorized into two learning styles from the perspective of transfer learning [101], [102]: multi-task learning and sequential learning. MTL involves learning different tasks simultaneously, while sequential learning involves learning different tasks in sequence. In learning models, catastrophic forgetting [103] often occurs, where after learning new knowledge, the model almost completely forgets previously learned content. In the field of AiOIR, since a single network is expected to restore images with multiple degradations, the model must learn knowledge related to various degradations, making catastrophic forgetting more likely. To enable the model to incrementally accumulate knowledge and avoid catastrophic forgetting, researchers proposed novel learning strategies, such as review learning [104] and sequential learning [105]. These methods are inspired by continual learning [106], [107] and replace mixed training (mixing datasets with different degradations) with sequential

training. It is worth noting that the learning order of multiple tasks is crucial for the quality of IR. In MiOIR [105], the authors study the effect of training order on the results and point out the impact of multi-task orders. In SimpleIR [104], the authors delve into the entropy difference distribution for various IR tasks. They propose determining the training dataset order based on abnormally high loss values and the intrinsic difficulty of tasks, measured by the entropy difference between original and degraded images. Recently, UniCoRN [108] topologically sorts both single and synthetic multi-degradation datasets based on a parent-child relationship graph and, further sort datasets within a level in the descending order of size to minimize the effect of catastrophic forgetting.

2) *Contrastive Learning*: One of the significant challenges in IR is effectively handling unseen tasks and degradation types. The vast variability in possible degradations can severely impede a model's generalization capabilities, making it less effective when confronted with new, unseen data. To address this issue, researchers have drawn inspiration from contrastive learning techniques that have proven successful in both high-level and low-level tasks [109]–[111]. Contrastive learning approaches typically serve as an additional form of regularization to improve the generalization of single-task restoration models [111]–[115]. By incorporating contrastive regularization, these methods aim to enhance model performance across a wide array of image restoration applications. In contrastive learning, the definitions of positive and negative samples can be flexibly adjusted, allowing researchers to tailor the learning process to better suit specific tasks and datasets. This flexibility ultimately enhances the model's adaptability and performance in diverse image restoration scenarios [84]. Moreover, contrastive learning-based loss functions have been proposed to obtain discriminative degradation representations in the latent space [54], [57], [89], [116], further improving the AiOIR model's ability to distinguish between different types of degradations and to generalize to unseen ones.

3) *Zero-shot Learning*: By restoring images with distortions that are absent in the training data, zero-shot image restoration tackles the challenge of generalizing effectively to unseen degradation types. For instance, methods (e.g., [117]–[120]) leverage pretrained diffusion models as generative priors, seamlessly integrating degraded images as conditions into the sampling process. In the case of AiOIR, MPerceiver [121] demonstrates strong zero-shot and few-shot capabilities across six unseen tasks. Additionally, TAO [122] employs test-time adaptation for AiOIR tasks, achieving results comparable to or better than traditional supervised methods. The core difficulty in these scenarios lies in the distribution shift between training and test data. This requires models to generalize beyond their training experience and adapt to previously unseen degradation types. Test-time adaptation (TTA) (e.g., [123]–[125]) has emerged as a key technique in addressing this issue, allowing models to dynamically adjust their parameters during the testing phase to better align with the characteristics of the degraded input images. By enabling the model to restore images with unknown degradations, zero-shot AiOIR aims to provide a more robust and versatile solution, making it a crucial step towards real-world applicability.

4) *Multi-task Learning*: MTL is a learning paradigm that leverages shared representations and knowledge across tasks, allowing models to learn more efficiently and effectively. By jointly learning from multiple objectives, MTL can improve generalization, reduce overfitting, and achieve better performance on individual tasks. Traditional MTL typically involves a combination of semantic tasks (e.g., classification, detection, segmentation). The tasks exhibit significant semantic differences and also possess distinct output spaces. Typical MTL architectures share a backbone and then branch into task-specific heads, while optimization techniques such as uncertainty weighting, GradNorm, or gradient surgery address conflicts between task gradients [126]–[128]. AiOIR, by contrast, treats each image degradation as a separate task but operates on the same input–output domain (*i.e.*, pixel-level image reconstruction). Losses remain largely reconstruction-focused (perceptual loss, pixel loss), and task conflicts arise at the gradient level, often manifesting as mutual interference among degradation models. The design of the degradation-aware module is often insufficient to resolve conflicts among different degradations. The optimization process often receives less attention, leading to an oversight of the complex relationships and potential conflicts between multiple degradations in mixed training scenarios. Unlike unified models (*e.g.*, [29], [54], [58], [105]) that employ mixed training, some novel studies address AiOIR from the perspective of MTL to resolve the inconsistencies and conflicts among different degradations, by treating each degradation as an independent task. By focusing on the optimization process and the interactions between tasks, these methods aim to mitigate conflicts and enhance overall performance. We can broadly classify AiOIR methods in MTL into two types: task grouping and task balancing.

Task Grouping. A notable example is GRIDS [129], which enhances MTL by strategically dividing tasks into optimal groups based on their correlations. Tasks that are highly related are grouped together, allowing for more effective training. GRIDS introduces an adaptive model selection mechanism that automatically identifies the most suitable task group during testing. This approach leverages the benefits of group training, ultimately improving overall performance by ensuring that related tasks are processed in a complementary manner.

Task Balancing. Conversely, Wu *et al.* [130] proposed a straightforward yet effective loss function that incorporates task-specific reweighting. This method dynamically balances the contributions of individual tasks, fostering harmony among diverse tasks. By adjusting the weight of each task based on specific characteristics and performance, this approach mitigates conflicts and enhances the overall effectiveness. Subsequently, Wu *et al.* proposed TUR [131], a task-aware optimization strategy that introduces adaptive task-specific regularization for AiOIR.

5) *Machine Unlearning*: Privacy protection is an increasingly critical issue in the field of artificial intelligence, particularly as models become more integrated into sensitive applications. One promising solution to address this challenge is machine unlearning [132]. This innovative approach aims to effectively erase the influence of private data from trained models, allowing them to function as if that sensitive information

was never utilized during the training process. Existing methodologies for unlearning can be broadly categorized into two types: exact unlearning [133], which seeks to completely eliminate the impact of specific data points, and approximate unlearning [134], which aims to diminish the influence of such data to a certain degree. While the concept of unlearning has been extensively explored in various contexts, including classification tasks and federated learning scenarios, its application in the realm of end-to-end IR remains largely uncharted.

To fill this gap, Su *et al.* [135] proposed an innovative framework that applied machine unlearning techniques to AiOIR models. They defined a scenario in which certain types of degradation are treated as private information that must be effectively forgotten by the model. Importantly, this process is designed to preserve the model’s performance on other types of degradations, ensuring that the overall functionality remains intact. To achieve this goal, the authors introduced a technique called instance-wise unlearning, which leveraged adversarial examples in conjunction with gradient ascent methods. This approach not only enhances the model’s ability to forget specific data but also maintains its robustness across various image restoration tasks.

C. Key Improvements of AiOIR

In addition to the network design in Sec. III-A and learning strategies in Sec. III-B, there are other key techniques to improve AiOIR models. In this section, we preliminarily categorize the key improvements of AiOIR models into the following four areas, *i.e.*, Prompt Learning, Mixture-of-Experts (MoE), Multimodal Model and Agentic IR System, which correspond to Sec. III-C1, Sec. III-C2, Sec. III-C3, Sec. III-C4, respectively. We also illustrate some other improvements, including deep unfolding methods, mask image modeling, hypernetworks, *etc.* For the sake of clarity, we list the representative works on all-in-one models based on the four types in Fig. 4.

1) *Prompt Learning*: Prompt learning, initially successful in natural language processing (NLP) [136]–[138], aims to tap into the knowledge that is inherent in the language model by providing instructions or relevant information. Inspired by the ability to effectively model task-specific context, prompts have been used for fine-tuning for vision tasks [139], [140]. To be specific, unlike single-task image restoration, learnable prompts enable better parameter-efficient adaptation of models facing multiple degradations. Recently, various prompts have been explored in AiOIR, as an adaptive lightweight module to encode degradation representation in the network. The core idea is to enable pretrained models to better understand and perform downstream tasks by constructing visual, textual or multimodal prompts, which are as follows.

Visual Prompting. Visual prompting has gained widespread attention for tackling both high-level and low-level vision tasks [141]–[143]. In AiOIR, prompt learning enables models to adaptively select task-specific prompts, achieving strong performance across diverse degradations. For example, AirNet [54] leverages degradation-aware features, while Tran-sweater [29] uses query-based guidance. This growing trend

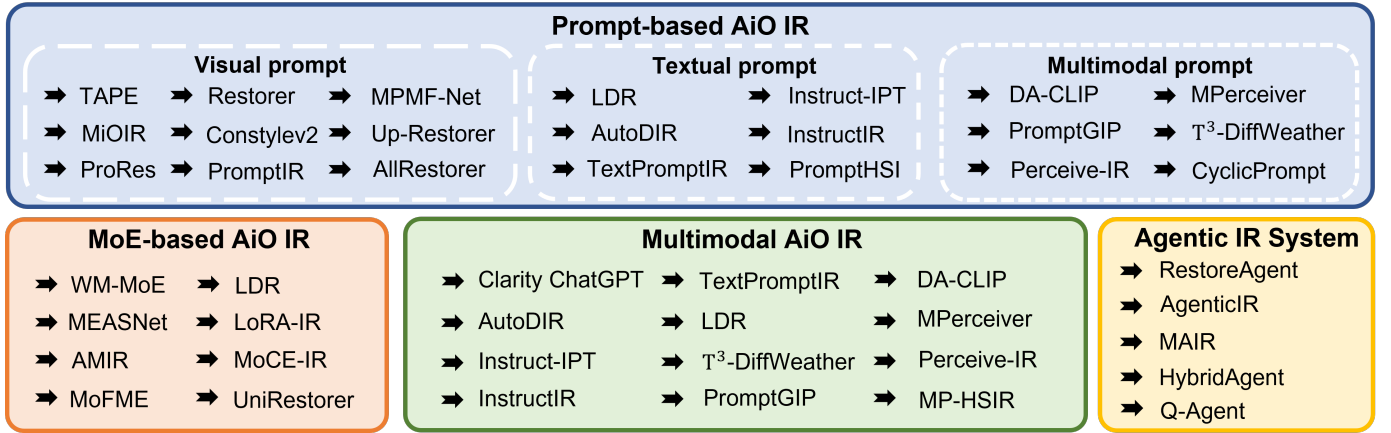


Fig. 4. The overview of AiOIR methods. This figure categorizes AiOIR into four types based on their key improvements, namely the Prompt-based models, MoE-based models, Multimodal models and Agentic IR systems.

highlights the increasing integration of prompt learning in AiOIR research.

PromptIR [58] is one of the most representative works, integrating a prompt block into the U-Net architecture to enhance Restormer [50]. The prompts serve as an adaptive, lightweight plug-and-play module as shown in Fig. 5, enabling multi-scale degradation-aware guidance across layers. Extending this idea, ProRes [59] embeds visual prompts directly into the input image. PromptGIP [96] proposes a training method similar to masked autoencoding [144], where certain portions of question and answer images are randomly masked. This prompts the model to reconstruct these patches from the unmasked areas. PIP [89] further introduces a novel Prompt-In-Prompt learning framework for AiOIR, which employs two innovative prompts: a degradation-aware prompt and a basic restoration prompt. To improve task-specific representation, Wen *et al.* [143] propose multi-axis prompt and multi-dimension fusion network for all-in-one traffic weather removal by incorporating prompts from three axes. CPL [116] establishes a new paradigm that extends contrastive learning principles from feature-level discrimination to the previously unexplored domain of prompt-level alignment. Recently, Wu *et al.* [145] introduce prompt distribution learning, which models prompts as distributions rather than fixed parameters.

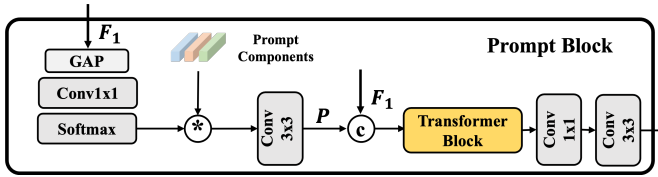


Fig. 5. Illustration of the prompt block in AiOIR.

Textual Prompting. While earlier AiOIR studies focused on learnable visual prompts, their effectiveness was limited by the semantic gap [146], making it difficult to accurately identify degradation types. To address this, recent works [61], [93]–[95], [99], [147] explore textual prompts for more precise and user-friendly guidance. For instance, TextPromptIR [93] leverages a fine-tuned BERT model to interpret task-specific

instructions, enabling semantic understanding of degradations. Text prompts allow users to describe degradations in natural language, enhancing model adaptability and accessibility. Building on this, Clarity ChatGPT [147] and AutoDIR [61] combine large language models with visual features to support intuitive and interactive IR, even in unseen tasks. Extending to hyperspectral image restoration, PromptHSI [74] introduces text-guided, frequency-aware modulation, showcasing the growing potential of language-driven AiOIR.

Multimodal Prompting. Vision-language models (VLMs) have shown strong potential in AiOIR by leveraging aligned visual and textual representations. Contrastive learning allows VLMs to train image and text encoders, thereby enabling prompts that integrate text for holistic semantics and vision for fine-grained details. Building on this, MPPerceiver [121] utilizes stable diffusion priors and CLIP-based dynamic prompts to adaptively handle diverse degradations. DA-CLIP [86] introduces an image controller to align degraded inputs with high-quality CLIP embeddings. CyclicPrompt [148] fuses CLIP-derived weather knowledge, conditional vectors, and textual prompts for context-aware restoration. MP-HSIR [75] focuses on HSI restoration by integrating spectral, visual, and textual prompts. Recently, VLU-Net [149] leverages CLIP-derived high-dimensional features for automatic selection of degradation-aware keys in deep unfolding networks. These works highlight multimodal prompting in enhancing adaptability and generalization in AiOIR.

2) *Mixture-of-Experts*: The mixture-of-experts (MoE) framework, first proposed in “Adaptive Mixture of Local Experts” [150], employs multiple specialized networks alongside a gating network that dynamically assigns weights to each expert based on the input. This architecture allows experts to focus on different data distributions, enhancing model specialization and performance in complex tasks. Researchers in AiOIR have observed that IR model parameters tend to be degradation-specific. For example, parameters related to one type of degradation are typically inactive when dealing with other types of degradation, and zeroing out these unrelated parameters has little impact on image restoration quality, as illustrated in LDR [99]. This observation aligns

with the concept of conditional computation in MoEs, where sparsity plays a key role. Applying MoEs to the field of AiOIR could lead to several improvements, including faster pretraining compared to dense models and quicker inference with the same number of parameters.

Yang *et al.* [99] proposed language-driven all-in-one adverse weather removal. This method generates degradation priors based on textual descriptions of weather conditions, which are then used to guide the adaptive selection of restoration experts. Similarly, WM-MoE [151] introduces a weather-aware routing mechanism to direct image tokens to specialized experts and employs multi-scale experts to handle diverse weather conditions. Both WM-MoE and MoFME [152] enhance IR tasks and downstream tasks like segmentation, while significantly reducing model parameters and inference time. In contrast, MEASNet [82] presents a novel multi-expert adaptive selection mechanism. This mechanism leverages both local and global image features to select the most appropriate expert models, effectively balancing task-specific demands and promoting resource sharing. More recently, MoCE-IR [153] introduces complexity experts with adaptive variable-size computational units that use a spring-inspired force mechanism to dynamically allocate experts. Building on similar principles, UniRestorer [154] construct a multi-granularity degradation set and a multi-granularity MoE restoration model. LoRA-IR [155] leverages a novel mixture of low-rank experts structure, combined with a CLIP-based degradation-guided router.

3) *Multimodal Model*: Multimodal learning has become increasingly pivotal in the domain of low-level vision [156], enabling the enrichment of visual understanding through the integration of diverse information sources. The fundamental objective of multimodal tasks is to learn potential feature representations from a multitude of modalities, such as textual captions and visual images, RGB images with supplementary components like depth or thermal images, and various forms of medical imaging data. Similarly, multimodal models in IR harness data from multiple sources to improve the fidelity and robustness of restored images. These models integrate complementary modalities to address limitations inherent in single-modality approaches, particularly in scenarios involving complex degradation. By leveraging different types of information, multimodal models enhance the structural details, texture, and overall quality of the restored image.

However, multimodal models also introduce challenges, including the increased computational complexity of handling diverse data streams and the requirement for well-aligned multimodal datasets. Additionally, the process of effectively fusing different types of data, which may have varying resolutions and characteristics, remains a significant technical hurdle. Here, we summarize various approaches to multimodal AiOIR methods (*e.g.*, Clarity-ChatGPT [147], AutoDIR [61], Instruct-IPT [95], InstructIR [94], *etc*). These involve the continuous guidance of IR via human language instructions, as well as the use of multimodal prompts for AiOIR, as previously mentioned. Clarity-ChatGPT is notable as the system that bridges adaptive image processing with interactive user feedback, innovatively integrating large language and visual models. AutoDIR automatically detects and restores

images with multiple unknown degradations by the semantic-agnostic blind image quality assessment (SA-BIQA). InstructIR [94] trains models using common image datasets and prompts generated by GPT-4, noting that this generalizes to human-written instructions. Moreover, CMAWRNet [157] leverages structure and texture decomposition images, and T³-DiffWeather [97] uses DepthAnything [98] features as a constraint for general prompts. Recently, Perceive-IR [84] leverages multi-level quality-driven prompts categorized into three tiers of quality by image-text pairs to perceive severity levels.

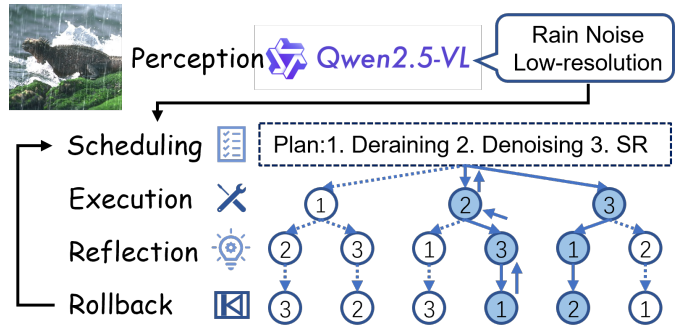


Fig. 6. Illustration of Agentic IR System.

4) *Agentic IR System*: The rise of Agentic IR Systems marks a paradigm shift in handling complex real-world degradations, positioning them as a natural extension of AiOIR [158], [159]. Powered by multimodal large language models (MLLMs), these systems enable autonomous analysis, dynamic planning, and adaptive model selection as shown in Fig. 6. For instance, RestoreAgent [160] introduces modular restoration guided by degradation-aware planning, while CoR [161] proposes a step-by-step chain-of-restoration strategy, albeit more suited for non-blind scenarios. Notably, AgenticIR [158] mimics human workflows through perception, scheduling, and adaptive execution using LLM-VLM collaboration. MAIR [162] structures degradation handling via a three-stage framework based on real-world priors, reducing the search space through expert agents. HybridAgent [163] further enhances efficiency by combining fast and slow agents, enabling ambiguity resolution while minimizing error propagation. More recently, Q-Agent [159] first fine-tunes MLLMs, and uses chain-of-thought to decompose multi-degradation perception. Collectively, these agentic approaches integrate reasoning, modularity, and prior knowledge to boost robustness and flexibility in multi-degradation restoration.

5) *Other Methods*: In addition to highlighting four key improvements, we also review other methods for AiOIR. Some models benefit from iterative algorithms in the deep unfolding networks (DUNs), and integrating the network design with pretrained mask image modeling (MIM) also holds significant potential. Meanwhile, hypernetworks with dynamically generated parameters are also highly suitable for AiOIR. The exploration of visual autoregressive modeling (VAR) as a novel paradigm for low-level vision tasks has recently extended to the field of AiOIR. The details are as follows.

TABLE I
SUMMARY OF USED DATASETS IN AiOIR TASKS.

Task	Dataset	Year	Training	Testing	Short Description	Type
Image Deblurring	GoPro [167]	2017	2103	1111	Blurred images at 1280x720	real
	HIDE [168]	2019	6397	2025	Blurry and sharp image pairs	real
	RealBlur [169]	2020	3758	980	182 different scenes	real
Image Denoising	Kodak [170]	1999	-	24	Lossless true color image suite	real
	Urban100 [171]	2015	-	100	100 images of urban scenes	real
	WED [172]	2016	4744	-	Images collected from Internet	real
	BSD400 [173]	2010	400	-	400 clean natural images	real
	CBSD68 [174]	2001	-	68	Images with different noisy levels	real
	McMaster [175]	2011	-	18	Crop size=500x500	real
Image Super-resolution	DIV2K [176]	2017	800	100	2K resolutions	real
	Flickr2K [177]	2017	2650	-	2K resolutions	real
	Set5 [178]	2012	-	5	Classic 5 images	real
	Set14 [179]	2012	-	14	Classic 14 images	real
	BSD100 [174]	2001	-	100	Objects, Natural images	real
	Urban100 [171]	2015	-	100	100 urban scenes	real
Shadow Removal	ISTD [180]	2018	1330	540	135 scenes with shadow mask images	synthetic
	SRD [181]	2017	2680	408	Large scale dataset for shadow removal	real
Image Desnowing	Snow100k [182]	2017	50000	50000	Including 1369 realistic snowy images	real and synthetic
	CSD [14]	2021	2000	-	A large-scale dataset called Comprehensive Snow Dataset	synthetic
	REVIDE [183]	2021	1698	284	Real-world Video Dehazing	real
	RealSnow+ [65]	2023	1650	240	Containing various resolutions	real
	KITTI-snow [184]	2023	50	-	Two intensity levels: severe and extremely severe	synthetic
Image Deraining	WeatherStream [30]	2023	176100	11400	Three weather conditions, <i>i.e.</i> , rain, snow, and fog	real
	RainDrop [185]	2018	1119	-	Various scenes and raindrops	real
	Outdoor-Rain [186]	2019	9000	1500	Degraded by both fog and rain streak	synthetic
	SPA [187]	2019	295000	1000	Various natural rain scenes	real
	Rain1400 [188]	2017	12600	1400	Diverse rainfall directions and levels	synthetic
Image Dehazing	Rain100L/H [189]	2017	200	100	Five rain streaks	synthetic
	Dense-Haze [190]	2019	33	-	Out-door hazy scenes	real
	RESIDE-OTS [191]	2019	313950	-	Outdoor training set	real
	RESIDE-ITS [191]	2019	110000	-	Indoor training set	synthetic
Low-light Image Enhancement	RESIDE-HSTS [191]	2019	-	20	Hybrid subjective testing set	synthetic and real
	LOL [192]	2018	485	15	Low- and normal-light images at 400x600	real

Deep Unfolding Methods. Under the framework of optimization theory and deep learning, DUNs enhance IR by unfolding iterative functions into end-to-end trainable architectures. Zhang *et al.* [164] proposed a DUN framework that integrates CNNs with model-based priors for task-specific IR. Given a degradation model, the clean image is estimated by minimizing an energy function. The half-quadratic splitting (HQS) algorithm [165] decomposes the optimization into two subproblems: one for the data fidelity term and the other for the prior. These subproblems are alternately solved, with the data term handled via least squares and the prior term approximated using CNNs. Building on this principle, DRM-IR [60] enhances the flexibility of all-in-one scenarios by introducing a reference-based and task-adaptive modeling paradigm. It establishes an efficient AiOIR framework that jointly models task-adaptive degradation and model-based restoration. Recently, Up-restore [166] employs a prompt-driven unrolling scheme inspired by ADMM and grounded in MAP estimation, effectively combining data-driven learning with physical priors. VLU-Net [149] leverages an automatic gradient estimation strategy based on VLMs, integrating multi-level information to improve feature preservation.

Large-scale Vision Models. Recent works have demonstrated the potential of pretrained vision-language models (VLMs) to enhance downstream tasks using generic visual and text representations [86], [193], [194]. A classic VLM typically consists of a text encoder and an image encoder, learning aligned multimodal features from image-text pairs through contrastive learning [86]. BLIP [194] improves this by eliminating noisy web data with synthetic captions. CLIP [86]

has demonstrated effective semantic alignment between vision and language, aiding numerous downstream tasks. In parallel, self-supervised models such as DINO [87] and DINO-v2 [88] have shown strong performance without requiring labeled data, further expanding the applicability of pretrained representations. VLMs have also gained significant traction in the domain of AiOIR [83]–[85], [195]. Perceive-IR [84] and DINO-IR [83] utilize the semantic prior knowledge and structural information mined by a DINO-based guidance module to enhance the restoration process. DA-CLIP [85] trains an additional controller that adapts the fixed CLIP image encoder to predict high-quality feature embeddings. AWRaCLE [196] employs visual in-context learning, incorporating the feature differences between the clean and degraded image pairs extracted by CLIP at the decoder.

Mask Image Modeling. Mask image modeling (MIM) (*e.g.*, [144], [197], [198]) is a technique in CV that involves training models to predict masked portions of images based on their surrounding context inspired by mask language modeling [199], [200]. This self-supervised approach reconstructs missing image regions, enhancing its visual representation learning. MIM has demonstrated effectiveness in visual tasks such as classification, detection, and segmentation. The MAE [144] framework effectively employs MIM to predict hidden tokens, showcasing impressive performance and generalization capabilities across a range of downstream tasks. Qin *et al.* [201] are the pioneers in introducing MIM into AiOIR, shifting the focus from degradation-type discrimination to intrinsic image information recovery. They proposed mask attribute conductance (MAC) to analyze each layer’s contri-

bution to resolving the input integrity gap and rank layers in descending order. DyNet [202] trains two variants (small and large) concurrently to reconstruct the clean image from masked degraded inputs. Notably, both variants share weights via an intra-network block-repetition scheme, reducing GPU hours by 50%. Most recently, Cat-AIR [203] introduces a content-aware and task-aware router that dynamically applies self-attention to complex regions and convolution to simpler ones, using learned masks to distinguish hard from easy patches within the feature map.

Hypernetworks. Hypernetworks [204] are a class of neural networks designed to generate parameters for other networks. This enables the network to dynamically adapt to varying input patterns, enhancing its flexibility. HAIR [205] introduces data-conditioned hypernetworks into the AiOIR by incorporating the plug-and-play modules into Restormer [50] to dynamically generate transformer block weights. Zhu *et al.* [206] propose MWFormer for multi-weather IR. A hypernetwork is employed to extract content-independent, weather-aware features. It also generates the weights and biases for feature vectors, along with parameters for depthwise convolutions and attention modules. Furthermore, it produces weather-informed feature vectors for both weather-type identification and the guidance of pretrained weather-specific models.

Visual Autoregressive. Tian *et al.* [207] proposed visual autoregressive modeling (VAR), a new generation paradigm that redefines the autoregressive learning and achieves efficiency and generative performance superior to stable diffusion [208]. For AiOIR, Varformer [209] explores the multi-scale representations learned by VAR and reveals its endogenous distribution alignment priors, which transition from global color information to fine-grained details. Unlike Varformer, which utilizes intermediate VAR features to guide a separate non-generative network, RestorerVAR [210] is generative. It fully exploits the strong priors of the pretrained VAR model by introducing degraded-image conditioning through cross-attention at each transformer block.

IV. EXPERIMENTS

To facilitate a comprehensive and effective comparison of various AiOIR methods, we begin by summarizing the key datasets, experimental settings, and evaluation metrics commonly used across different tasks. Following this, we conduct a detailed comparison of existing benchmarks across several representative image restoration tasks, such as low-light enhancement, dehazing, deblurring, denoising, deraining, and desnowing. This structured schema ensures a thorough evaluation of the performance and capabilities of different all-in-one image restoration methods.

A. Datasets and Evaluation Metrics

Datasets. A wide range of datasets are available for AiOIR, varying significantly in terms of image quantity, quality, resolution, and diversity. Tab. I summarizes the datasets used for different AiOIR tasks. Recently, FoundIR [211] contributes a million-scale high-quality dataset for IR foundational model, highlighting the potential of AiOIR in real-world scenarios.

Evaluation Metrics. The performance of AiOIR methods is typically evaluated using three aspects of metrics: Distortion metrics(*e.g.*, PSNR, SSIM [212]) refer to the relationship between the restored image and the original image. Perceptual metrics(*e.g.*, FID [213], LPIPS [214]) evaluate how much the image appears like a natural image. No-reference metrics(*e.g.*, NIQE [215], BRISQUE [216]) are commonly based on estimating deviations from natural image statistics. In addition, there are several metrics that play a crucial role in comparing the performances of different AiOIR methods, including IL-NIQE [32], NIMA [217], CLIP-IQA [218], LOE [219], Consistency [220], PI [215], and MUSIQ [221].

B. Experiments and Analysis

To demonstrate the superiority of different AiOIR models, we provide an objective quality comparison in Tab. II, Tab. III, Tab. IV, Tab. V, Tab. VI. The evaluation metrics are composed of PSNR, SSIM [212]. Specifically, we summarize the experimental results of different methods under five common experimental settings in the field of AiOIR, *i.e.*, *Setting1* for three-degradation scenarios in Tab. II: dehazing, deraining, denoising (the noise level $\sigma = 15, \sigma = 25, \sigma = 50$), *Setting2* for five-degradation scenarios in Tab. III: dehazing, deraining, denoising (the noise level $\sigma = 25$), deblurring, and low-light enhancement, *Setting3* for synthetic weather-related scenarios (the All-Weather dataset [29]) in Tab. IV: snow, rain+fog and raindrop, *Setting4* for real-world weather-related scenarios in Tab. V: haze, rain and snow, and *Setting5* for mixed-degradation scenarios (the CDD-11 dataset [31]) in Tab. VI: low-light, haze, rain, snow, low+haze, low+rain, low+snow, haze+rain, haze+snow, low+haze+rain, and low+haze+snow. The results align closely with the original paper.

For *Setting1* in Tab. II, ABAIR [234] and DFPIR [243] achieve the highest average performance both without and with the assistance of foundational models, respectively, indicating strong generalization across diverse degradations. ABAIR attains an average PSNR/SSIM of 32.91/0.920, while DFPIR follows closely with 32.88/0.919, underscoring that careful model design and training strategies are as crucial as leveraging VLMs. For dehazing, ABAIR also achieves the highest PSNR of 33.53, significantly outperforming others, followed by DaAIR [230] at 32.30 and PIP [89] at 32.09. MTAIR [235] and MEASNet [82] stand out with the highest PSNR values of 39.15 and 39.00 for deraining, respectively. Many recent models adopt complex mechanisms such as frequency-aware transformations [232], optimal transport [233], deep unfolding networks [149], and hypernetwork-based architectures [205], suggesting a growing emphasis on specialized designs to tackle varying degradation patterns.

For *Setting2* in Tab. III, D³Net [244] achieves the best average performance across tasks, particularly excelling in dehazing and low-light enhancement. ABAIR and DFPIR also show strong results, with high average scores, indicating their robustness across multiple degradation types. Prompt-based models such as CPL_{PromptIR} [116] and CyclicPrompt [148] are among the top performers, suggesting that prompt learning strategies remain a dominant paradigm for tackling multiple

TABLE II
PERFORMANCE COMPARISONS OF AIOIR MODELS ON THREE CHALLENGING DATASETS.

	Method	Venue & Year	Params	Dehazing	Deraining	Denoising on BSD68 dataset [174]			Average	Approach
				SOTS [191]	Rain100L [189]	$\sigma = 15$	$\sigma = 25$	$\sigma = 50$		
Single	LPN [222]	CVPR'19	3M	20.84/0.828	24.88/0.784	26.47/0.778	24.77/0.748	21.26/0.552	23.64/0.738	Specific
	ADFNet [223]	AAAI'23	8M	28.13/0.961	34.24/0.965	33.76/0.929	30.83/0.871	27.75/0.793	30.94/0.904	Specific
	DehazeFormer [224]	TIP'23	25M	29.58/0.970	35.37/0.969	33.01/0.914	30.14/0.858	27.37/0.779	31.09/0.898	Specific
	DRSFormer [19]	CVPR'23	34M	29.02/0.968	35.89/0.970	33.28/0.921	30.55/0.862	27.58/0.786	31.26/0.902	Specific
Multiple	MPRNet [225]	CVPR'21	16M	28.00/0.958	33.86/0.958	33.27/0.920	30.76/0.871	27.29/0.761	30.63/0.894	General
	Restormer [50]	CVPR'22	26M	27.78/0.958	33.78/0.958	33.72/0.865	30.67/0.865	27.63/0.792	30.75/0.901	General
	NAFNet [52]	ECCV'22	17M	24.11/0.960	33.64/0.956	33.18/0.918	30.47/0.865	27.12/0.754	29.67/0.844	General
	FSNet [226]	TPAMI'23	13M	29.14/0.969	35.61/0.969	33.81/0.874	30.84/0.872	27.69/0.762	31.42/0.906	General
All-in-One	MambaIR [227]	ECCV'24	27M	29.57/0.970	35.42/0.969	33.88/0.931	30.95/0.874	27.74/0.793	31.51/0.907	General
	DL [228]	TPAMI'19	2M	26.92/0.931	32.62/0.931	33.05/0.914	30.41/0.861	26.90/0.740	29.98/0.875	parameterized image operator
	TKMANet [63]	CVPR'22	29M	30.41/0.973	34.94/0.972	33.02/0.924	30.31/0.820	28.80/0.554	30.50/0.849	two-stage knowledge learning
	AirNet [54]	CVPR'22	9M	27.94/0.962	34.90/0.967	33.92/0.933	31.26/0.888	28.00/0.797	31.20/0.910	contrastive-based°radation-guided
Prompt	PIP _{restomer} [89]	arXiv'23	27M	32.09/0.981	38.29/0.984	34.24/0.936	31.60/0.893	28.35/0.806	32.91/0.920	prompt-in-prompt learning
	IDR [57]	CVPR'23	15M	29.87/0.970	36.03/0.971	33.89/0.931	31.32/0.884	28.04/0.798	31.83/0.911	ingredient-oriented learning
	PromptIR [58]	NeurIPS'23	36M	30.58/0.974	36.37/0.972	33.98/0.933	31.31/0.888	28.06/0.799	32.06/0.913	prompt for AIOIR
	Gridformer [67]	IJCV'23	34M	30.37/0.970	37.15/0.972	33.93/0.931	31.37/0.887	28.11/0.801	32.19/0.912	transformer with grid structure
Prompt	ProRes [59]	arXiv'23	371M	28.38/0.938	33.68/0.954	32.10/0.907	30.18/0.863	27.58/0.779	30.38/0.888	degradation-aware visual prompt
	NDR [62]	TIP'24	28M	28.64/0.962	35.42/0.969	34.01/0.932	31.36/0.887	28.10/0.798	31.51/0.910	neural degradation representation
	ArtPromptIR [130]	ACM MM'24	36M	30.83/0.979	37.94/0.982	34.06/0.934	31.42/0.891	28.14/0.801	32.49/0.917	via multi-task collaboration
	AnyIR [229]	arXiv'24	6M	31.38/0.979	37.90/0.981	33.95/0.933	31.29/0.889	28.03/0.797	32.51/0.916	local-global gated intertwining
Prompt	DaAIR [230]	arXiv'24	6M	32.30/0.981	37.10/0.978	33.92/0.930	31.26/0.884	28.00/0.792	32.51/0.913	efficient degradation-aware
	MEASNet [82]	arXiv'24	31M	31.61/0.981	39.00/0.985	34.12/0.935	31.46/0.892	28.19/0.803	32.85/0.919	multi-expert adaptive selection
	U-WADN [231]	arXiv'24	6M	29.21/0.971	35.36/0.968	33.73/0.931	31.14/0.886	27.92/0.793	31.47/0.910	unified-width adaptive network
	Shi <i>et al.</i> [232]	arXiv'24	-	29.20/0.972	37.50/0.980	34.59/0.941	31.83/0.900	28.46/0.814	32.32/0.921	frequency-aware transformers
Prompt	DyNet [202]	arXiv'24	16M	31.98/0.981	38.71/0.983	34.11/0.936	31.44/0.892	28.18/0.803	32.88/0.920	dynamic pre-training
	Hair [205]	arXiv'24	29M	30.98/0.979	38.59/0.983	34.16/0.935	31.51/0.892	28.24/0.803	32.70/0.919	hypernetworks-based
	LoRA-IR [155]	arXiv'24	-	30.68/0.961	37.75/0.979	34.06/0.937	31.42/0.891	28.18/0.803	32.42/0.914	mixture of low-rank experts
	Up-Restorer [166]	AAAI'25	28M	30.68/0.977	36.74/0.978	33.99/0.933	31.33/0.888	28.07/0.799	32.16/0.915	ADMM-solver-based design
Prompt	TURPromptIR [131]	AAAI'25	36M	31.17/0.978	38.57/0.984	34.06/0.932	31.40/0.887	28.13/0.797	32.67/0.916	a novel loss function
	AdaIR [79]	ICLR'25	29M	31.06/0.980	38.64/0.983	34.12/0.935	31.45/0.892	28.19/0.802	32.69/0.918	frequency mining and modulation
	DA-RCOT [233]	TPAMI'25	50M	31.26/0.977	38.36/0.983	33.98/0.934	31.33/0.890	28.10/0.801	32.60/0.917	as an optimal transport problem
	AAIR [234]	arXiv'24	41M	33.53/0.984	38.69/0.982	34.18/0.935	31.38/0.890	28.25/0.804	32.31/0.919	a three-phase approach
Prompt	MoCE-IR [153]	CVPR'25	25M	31.34/0.979	38.57/0.984	34.11/0.932	31.45/0.888	28.18/0.800	32.73/0.917	mixture-of-complexity-experts framework
	MTAIR [235]	arXiv'24	-	31.34/0.983	39.15/0.984	34.14/0.936	31.50/0.893	28.24/0.805	32.87/0.920	Mamba-Transformer cross-dimensional
	DCPTPromptIR [236]	ICLR'25	35M	31.91/0.981	38.43/0.983	34.17/0.933	31.53/0.889	28.30/0.802	32.87/0.918	learn to classify degradation
	RamIR [237]	APP' INTELL'25	22M	31.29/0.977	38.16/0.981	34.04/0.931	31.61/0.891	28.19/0.801	32.65/0.916	prompt-driven Mamba-based
Prompt	Cat-AIR [203]	arXiv'25	-	31.49/0.980	38.43/0.983	34.11/0.935	31.44/0.892	28.14/0.803	32.72/0.919	content and task-aware framework
	DSwinIR [238]	arXiv'25	24M	31.86/0.980	37.73/0.983	34.12/0.933	31.59/0.890	28.31/0.803	32.72/0.917	deformable sliding window transformer
	CPLPromptIR [116]	arXiv'25	36M	31.27/0.980	38.77/0.985	34.15/0.933	31.50/0.889	28.23/0.800	32.78/0.917	contrastive prompt regularization
	AnyIR [239]	arXiv'25	6M	31.75/0.981	38.61/0.984	34.12/0.936	31.46/0.893	28.20/0.804	32.83/0.920	local-global gated mechanism
Prompt	MIRAGE [240]	arXiv'25	10M	31.86/0.981	38.94/0.985	34.12/0.935	31.46/0.891	28.19/0.803	32.91/0.919	within the SPD manifold space
	BaryIR [241]	arXiv'25	-	31.33/0.980	38.95/0.984	34.16/0.935	31.54/0.892	28.25/0.802	32.85/0.919	in continuous barycenter space
	SIPL_PromptIR [242]	arXiv'25	39M	31.09/0.977	38.43/0.984	34.12/0.933	31.48/0.889	28.22/0.800	32.67/0.917	privilege learning
	TextPromptIR [93] $\star \oplus$	arXiv'23	124M+110M	31.65/0.978	38.41/0.982	34.17/0.936	31.52/0.893	28.26/0.805	32.80/0.919	textual prompt for AIOIR
Prompt	InstructIR-3D [94] $\star \oplus$	ECCV'24	16M+17M	30.22/0.959	37.98/0.978	34.15/0.933	31.52/0.890	28.30/0.804	32.43/0.913	natural language prompts
	DA-CLIP _{IR-SDE} [85] \star	ICLR'24	49M+125M	26.83/0.962	35.85/0.972	31.43/0.889	25.05/0.605	18.33/0.308	27.50/0.747	degradation-aware vision-language model
	Perceive-IR [84] \star	arXiv'24	42M+86M	30.87/0.975	38.29/0.980	34.13/0.934	31.53/0.890	28.31/0.804	32.63/0.917	quality-aware degradation
	VLU-Net [149] \star	CVPR'25	35M+88M	30.71/0.980	38.93/0.984	34.13/0.935	31.48/0.892	28.23/0.804	32.70/0.919	vision-language gradient descent-driven
Prompt	DFPIR [243] $\star \oplus$	CVPR'25	31M+63M	31.87/0.980	38.65/0.982	34.14/0.935	31.47/0.893	28.25/0.806	32.88/0.919	degradation-aware feature perturbation

Note: The dash (“-”) in the “Params” column indicates that there is no corresponding source code. \star denotes models assisted by foundation models (e.g., CLIP, BERT, or DINO); \oplus denotes models assisted by additional modalities (e.g., text or depth). These notations are consistent across all subsequent tables.

degradations simultaneously. Degradation-awareness remains crucial, with models like DaAIR and Perceive-IR [84] tailoring the restoration process to specific degradation characteristics and yielding excellent performance. The trade-off between model size and performance is also evident. Lightweight designs such as TAPE [245] achieve competitive results in certain tasks, whereas more complex architectures like Gridformer [67] deliver more reliable performance across all tasks. For *Setting3* in Tab. IV, MODEM [256] achieves the strongest overall performance by the Morton-order 2D-selective-scan module, with an average PSNR/SSIM of 32.87/0.938. It is closely followed by DSwinIR [238] and LoRA-IR [155], which deliver averages of 32.74/0.943 and 32.76/0.941, respectively, demonstrating the effectiveness of deformable window attention and mixture-of-experts. By contrast, early methods such as All-in-One [53] yield a much lower average PSNR of 28.05 dB, highlighting the substantial gains achieved by these newer, specialized architectures. For *Setting4* in Tab. V, although Transweather [29] carries

the larger parameter count, it struggles to deliver competitive performance. In contrast, though more parameter-efficient, AirNet still falls short in overall restoration quality in the WeatherStream dataset. TKMANet [63] and WGWS-Net [65] show a notable improvement in both metrics, balancing effectiveness and efficiency. Zhu *et al.* [65] first construct the Real-World Dataset for image restoration under multiple weather conditions of real scenes. Specifically, we test on SPA+ [187] for deraining, RealSnow [65] for desnowing, and REVIDE [183] for dehazing. DSwinIR achieves superior performance on this dataset. Overall, these results demonstrate a clear progression in multi-weather restoration, suggesting that the field is advancing towards more sophisticated and robust techniques across diverse conditions.

For *Setting5* in Tab. VI, we categorize existing methods into four settings: (a) One-to-One trains on isolated degradations; (b) One-to-Many trains on multiple isolated degradations and tests on them jointly; (c) One-to-Composite trains and tests on both isolated and composite degradations; and (d) Step-by-

TABLE III

PERFORMANCE COMPARISONS OF AIOIR MODELS ON FIVE CHALLENGING DATASETS. DENOISING RESULTS ARE REPORTED FOR THE NOISE LEVEL $\sigma = 25$.

	Method	Venue & Year	Params	Dehazing	Deraining	Denoising	Deblurring	Low-light	Average	Approach
Single	ADFNet [223]	AAAI'23	8M	24.18/0.928	32.97/0.943	31.15/0.882	25.79/0.781	21.15/0.823	27.05/0.871	Specific
	DehazeFormer [224]	TIP'23	25M	25.31/0.937	33.68/0.954	30.89/0.880	25.93/0.785	21.31/0.819	27.42/0.875	Specific
	DRSformer [19]	CVPR'23	34M	24.66/0.931	33.45/0.953	30.97/0.881	25.56/0.780	21.77/0.821	27.28/0.873	Specific
	HI-Diff [246]	NeurIPS'23	24M	25.09/0.935	33.26/0.951	30.61/0.878	26.48/0.800	22.01/0.870	27.49/0.887	Specific
Multiple	Retinexformer [247]	ICCV'23	2M	24.81/0.933	32.68/0.940	30.84/0.880	25.09/0.779	22.76/0.863	27.24/0.873	Specific
	SwinIR [248]	ICCVW'21	1M	21.50/0.891	30.78/0.923	30.59/0.868	24.52/0.773	17.81/0.723	25.04/0.835	General
	MIRNet-v2 [249]	TPAMI'22	6M	24.03/0.927	33.89/0.954	30.97/0.881	26.30/0.799	21.52/0.815	27.34/0.875	General
	DGUNet [250]	CVPR'22	17M	24.78/0.940	36.62/0.971	31.10/0.883	27.25/0.837	21.87/0.823	28.32/0.891	General
	Restormer [50]	CVPR'22	26M	24.09/0.927	34.81/0.960	31.49/0.884	27.22/0.829	20.41/0.806	27.60/0.881	General
	NAFNet [52]	ECCV'22	17M	25.23/0.939	35.56/0.967	31.02/0.883	26.53/0.808	20.49/0.809	27.76/0.881	General
	FSNet [226]	TPAMI'23	13M	25.53/0.943	36.07/0.968	31.33/0.883	28.32/0.869	22.29/0.829	28.71/0.898	General
All-in-One	MambalR [227]	ECCV'24	27M	25.81/0.944	36.55/0.971	31.41/0.884	28.61/0.875	22.49/0.832	28.97/0.901	General
	DL [228]	TPAMI'19	2M	20.54/0.826	21.96/0.762	23.09/0.745	19.86/0.672	19.83/0.712	21.05/0.743	parameterized image operator
	Transweather [29]	CVPR'22	38M	21.32/0.885	29.43/0.905	29.00/0.841	25.12/0.757	21.21/0.792	25.22/0.836	weather type queries
	TAPE [245]	ECCV'22	1M	22.16/0.861	29.67/0.904	30.18/0.855	24.47/0.763	18.97/0.621	25.09/0.801	task-agnostic prior
	AirNet [54]	CVPR'22	9M	21.04/0.884	32.98/0.951	30.91/0.882	24.35/0.781	18.18/0.735	25.49/0.846	contrastive-based°radation-guided
	IDR [57]	CVPR'23	15M	25.24/0.943	35.63/0.965	31.60/0.887	27.87/0.846	21.34/0.826	28.34/0.893	ingredient-oriented learning
	PIPRestorer [89]	arXiv'23	27M	32.11/0.979	38.09/0.983	30.94/0.877	28.61/0.861	24.06/0.859	30.81/0.901	prompt-in-prompt learning
	PromptIR [58]	NeurIPS'23	36M	26.54/0.949	36.37/0.970	31.47/0.886	28.71/0.881	22.68/0.832	29.15/0.904	prompt for AIOIR
	DASLMPRNet [251]	arXiv'23	15M	25.82/0.947	38.02/0.980	31.57/0.890	26.91/0.823	20.96/0.826	28.66/0.893	decomposition ascribed synergistic
	Gridformer [67]	IJCV'23	34M	26.79/0.951	36.61/0.971	31.45/0.885	29.22/0.884	22.59/0.831	29.33/0.904	transformer with grid structure
All-in-One	ArtPromptIR [130]	ACM MM'24	36M	29.93/0.908	22.09/0.891	29.43/0.843	25.61/0.776	21.99/0.811	25.81/0.846	via multi-task collaboration
	DaAIR [230]	arXiv'24	6M	31.97/0.980	36.28/0.975	31.07/0.878	29.51/0.890	22.38/0.825	30.24/0.910	efficient degradation-aware
	AnyIR [229]	arXiv'24	6M	29.84/0.977	36.91/0.977	31.15/0.882	26.86/0.822	23.50/0.845	29.65/0.901	local-global gated intertwining
	MEASNet [82]	arXiv'24	31M	31.05/0.980	38.32/0.982	31.40/0.888	29.41/0.890	23.00/0.845	30.64/0.917	multi-expert adaptive selection
	Hair [205]	arXiv'24	29M	30.62/0.978	38.11/0.981	31.49/0.891	28.52/0.874	23.12/0.847	30.37/0.914	hypernetworks-based
	TURTransweather [131]	AAAI'25	38M	29.68/0.966	33.09/0.957	30.40/0.869	26.63/0.815	23.02/0.838	28.56/0.888	a novel loss function
	AdaIR [79]	ICLR'25	29M	30.53/0.978	38.02/0.981	31.35/0.889	28.12/0.858	23.00/0.845	30.20/0.910	frequency mining and modulation
	DA-RCOT [233]	TPAMI'25	50M	30.96/0.975	37.87/0.980	31.23/0.888	28.68/0.872	23.25/0.836	30.40/0.911	as an optimal transport problem
	ABAIR [234]	arXiv'24	41M	33.46/0.983	38.18/0.983	31.38/0.898	29.00/0.878	24.20/0.865	31.24/0.921	a three-phase approach
	MoCE-IR [153]	CVPR'25	25M	30.48/0.974	38.04/0.982	31.34/0.887	30.05/0.899	23.00/0.852	30.58/0.919	mixture-of-complexity-experts framework
All-in-One	DCPTPromptIR [236]	ICLR'25	35M	30.72/0.977	37.32/0.978	31.32/0.885	28.84/0.877	23.35/0.840	30.31/0.911	learn to classify degradation
	RamIR [237]	APPL INTELL'25	22M	31.09/0.978	37.56/0.979	31.44/0.886	28.82/0.878	22.02/0.828	30.18/0.910	prompt-driven Mamba-based
	D ³ Net [244]	arXiv'25	38M	32.57/0.965	38.35/0.973	31.73/0.860	26.49/0.857	23.36/0.901	cross-domain and dynamic decomposition	
	Cat-AIR [203]	arXiv'25	-	30.88/0.978	38.21/0.982	31.38/0.890	28.91/0.876	23.46/0.848	30.57/0.915	content and task-aware framework
	DSwinIR [238]	arXiv'25	24M	30.09/0.975	37.77/0.982	31.34/0.885	29.17/0.879	22.64/0.843	30.19/0.913	deformable sliding window transformer
	CPLPromptIR [116]	arXiv'25	36M	30.82/0.978	38.20/0.983	31.41/0.887	28.72/0.878	23.65/0.855	30.55/0.915	contrastive prompt regularization
	AnyIR [239]	arXiv'25	6M	31.41/0.980	38.51/0.983	31.37/0.891	28.85/0.883	23.11/0.856	30.65/0.919	local-global gated mechanism
	MIRAGE [240]	arXiv'25	10M	31.45/0.980	38.92/0.985	31.41/0.892	28.10/0.858	23.59/0.858	30.68/0.914	within the SPD manifold space
	BaryIR [241]	arXiv'25	-	31.12/0.976	38.05/0.981	31.43/0.891	29.30/0.888	23.38/0.852	30.66/0.918	in continuous barycenter space
	InstructIR-5D [94] ★⊕	ECCV'24	16M+17M	36.84/0.973	37.10/0.956	31.40/0.887	29.40/0.886	23.00/0.836	29.55/0.907	natural language prompts
All-in-One	Perceive-IR [84] ★	TIP'25	42M+86M	28.19/0.964	37.25/0.977	31.44/0.887	29.46/0.886	22.88/0.833	29.84/0.909	quality-aware degradation
	VLU-Net [149] ★	CVPR'25	35M+88M	30.84/0.980	38.54/0.982	31.43/0.891	27.46/0.840	22.29/0.833	30.11/0.905	vision-language gradient descent-driven
	DFPIR [243] ★⊕	CVPR'25	31M+63M	31.64/0.979	37.62/0.978	31.29/0.889	28.82/0.873	23.82/0.843	30.64/0.913	degradation-aware feature perturbation
	CyclicPrompt [148] ★⊕	arXiv'25	30M+486M	33.02/0.983	37.03/0.989	31.33/0.941	29.42/0.925	21.79/0.837	30.52/0.935	cyclic prompt-driven universal framework

TABLE IV

PERFORMANCE COMPARISONS OF AIOIR MODELS ON ALL-WEATHER DATASET [29]. BELOW THE DIVIDING LINE IN THE TABLE IS AIOIR METHODS.

Method	Snow	Rain+Fog	Raindrop	Average	Params
SwinIR [248]	28.18/0.880	23.23/0.869	30.82/0.904	27.41/0.884	12M
MPRNet [29]	28.66/0.869	30.25/0.914	30.99/0.916	29.30/0.900	16M
Restormer [50]	29.37/0.881	29.22/0.907	31.21/0.919	29.93/0.902	26M
All-in-One [53]	28.33/0.882	24.71/0.898	31.12/0.927	28.05/0.902	44M
Transweather [29]	29.31/0.888	28.83/0.900	30.17/0.916	29.44/0.901	38M
AirNet [54]	27.92/0.858	23.12/0.837	28.23/0.892	26.42/0.862	9M
WGWS-Net [65]	28.91/0.856	28.29/0.928	32.01/0.925	30.07/0.901	6M
WeatherDiff [64]	30.09/0.904	29.64/0.931	30.71/0.931	30.15/0.922	83M
TKMANet [63]	30.24/0.902	29.92/0.917	30.99/0.927	30.38/0.915	29M
UtilityIR [252]	29.47/0.879	31.16/0.927	32.01/0.925	30.88/0.910	26M
AWRPC [66]	31.92/0.934	31.39/0.933	31.93/0.931	31.75/0.933	-
Histoformer [253]	32.16/0.926	32.08/0.939	33.06/0.944	32.43/0.936	17M
LoRA-IR [155]	32.28/0.930	32.62/0.945	33.39/0.949	32.76/0.941	-
T ³ -DiffWeather [97] ★⊕	32.37/0.936	31.99/0.937	32.66/0.941	32.34/0.938	69M+25M
MWFormer [206]	30.92/0.908	30.27/0.912	31.91/0.927	31.03/0.916	170M
TURTransweather [131]	30.62/0.909	29.75/0.907	31.61/0.933	30.66/0.916	38M
CyclicPrompt [148] ★⊕	32.16/0.927	32.81/0.937	32.57/0.945	32.51/0.936	30M+486M
DSwinIR [238]	32.58/0.931	32.76/0.950	32.88/0.947	32.74/0.943	24M
DA ² Diff [254]	31.42/0.916	31.58/0.939	33.01/0.945	31.67/0.933	-
HOGformer [255]	32.41/0.930	32.89/0.946	32.72/0.945	32.67/0.940	17M
CPLPromptIR [116]	32.27/0.928	32.16/0.942	32.73/0.943	32.39/0.938	36M
MODEM [256]	32.52/0.929	33.10/0.941	33.01/0.943	32.87/0.938	20M

Step trains on isolated degradations and tests on their combinations step by step. Among the One-to-Composite methods, OneRestore [31], which introduces a novel dataset CDD-11 encompassing both single and composite degradations, achieves a good balance between accuracy and efficiency.

TABLE V

PERFORMANCE COMPARISONS OF AIOIR MODELS ON REAL-WORLD WEATHER-RELATED DATASETS.

Method	the WeatherStream Dataset [30]			Params	
	Haze	Rain	Snow		
NAFNet [52]	22.20/0.803	23.01/0.803	22.11/0.826	22.44/0.811	17M
GRL [258]	22.88/0.802	23.75/0.805	22.59/0.829	23.07/0.812	3M
Restormer [50]	22.90/0.803	23.67/0.804	22.51/0.828	22.86/0.812	26M
MPRNet [225]	21.73/0.763	21.50/0.791	20.74/0.801	21.32/0.785	16M
Transweather [29]	22.55/0.774	22.21/0.772	21.79/0.792	22.18/0.779	38M
AirNet [54]	21.56/0.770	22.52/0.797	21.44/0.812	21.84/0.793	9M
TKMANet [63]	22.38/0.805	23.22/0.795	22.25/0.827	22.62/0.809	29M
WGWS-Net [65]	22.78/0.800	23.80/0.807	22.72/0.831	23.10/0.813	6M
the Real-World Dataset [65]					
	20.10/0.85	37.32/0.97	29.37/0.88	28.93/0.90	29M
	17.33/0.82	33.64/0.93	26.92/0.86	26.71/0.86	38M
	20.38/0.88	39.78/0.98	29.72/0.91	29.96/0.92	38M
	29.46/0.85	38.94/0.98	33.61/0.93	34.01/0.92	6M
DSwinIR [238]	30.14/0.89	40.60/0.98	33.80/0.93	34.85/0.93	24M

In comparison, the AllRestorer model [257] achieves the best performance by adaptive weights and composite

TABLE VI
PERFORMANCE COMPARISON ON CDD-11 DATASET. METHODS ARE CATEGORIZED INTO ONE-TO-ONE, ONE-TO-MANY, AND ONE-TO-COMPOSITE.

Type	Method	Venue & Year	PSNR ↑	SSIM ↑	Params
One-to-One	MPRNet [225]	CVPR'21	25.47	0.856	16M
	MIRNet2 [249]	TPAMI'22	25.37	0.854	6M
	Restormer [50]	CVPR'22	26.99	0.865	26M
	DGUNet [250]	CVPR'22	25.33	0.844	18M
	NAFNet [52]	ECCV'22	26.22	0.796	17M
	SRUDC [259]	ICCV'23	27.64	0.860	7M
	Fourmer [260]	ICML'23	23.44	0.789	6M
One-to-Many	OKNet [261]	AAAI'24	26.33	0.861	6M
	AirNet [54]	CVPR'22	23.75	0.814	9M
	TransWeather [29]	CVPR'22	23.13	0.804	38M
	WeatherDiff [64]	TPAMI'23	24.09	0.799	83M
	PromptIR [58]	NeurIPS'23	25.90	0.850	36M
	WGWS-Net [65]	CVPR'23	26.96	0.861	6M
	HAIR [205]	arXiv'24	27.85	0.866	29M
One-to-Composite	OneRestore [31]	ECCV'24	28.47	0.878	6M
	AllRestorer [257] ★ ⊕	arXiv'24	33.72	0.944	12M+88M
	DA-CLIPAFNNet ★	ICLR'24	26.56	0.860	86M+125M
	MoCE-IR-S [153]	CVPR'25	29.05	0.881	11M
	DCPT _{NAFNet} [236]	ICLR'25	28.84	0.891	68M
Step-by-Step	VL-UR [262] ★	arXiv'25	28.76	0.879	-
	MIRAGE [240]	arXiv'25	29.33	0.887	10M
Step-by-Step	CoR _{HAIR} [161]	arXiv'24	28.33	0.869	30M
	CoR _{OneRestore} [161]	arXiv'24	28.84	0.879	8M

V. CHALLENGES AND FUTURE DIRECTIONS

A. Challenges

AiOIR models encounter several challenges that limit their effectiveness in real-world applications. Task conflicts arise from differing objectives in denoising, deblurring, and dehazing, complicating simultaneous optimization and leading to inconsistent performance. Additionally, these models struggle with out-of-distribution (OOD) degradations, as real-world images often exhibit a mix of degradation types that do not align with training data. The computational demands of current models hinder deployment on resource-constrained devices, necessitating a balance between restoration quality and efficiency. Furthermore, the reliance on large-scale, high-quality labeled real-world datasets poses challenges due to the resource-intensive nature of data acquisition, resulting in generalization issues. Lastly, most models focus on RGB images, while handling high-dimensional data introduces further complexities, such as increased dimensionality and temporal consistency requirements. Addressing these challenges is essential for improving AiOIR models' practicality and performance.

1) *Task Conflicts*: In AiOIR, task conflicts arise due to differing objectives across various tasks like denoising, deblurring, and dehazing. Tasks may require opposite optimizations—denoising reduces high-frequency noise, while deblurring enhances high-frequency details. Additionally, data characteristics for different tasks vary, leading to inconsistent performance when training on multiple tasks.

2) *OOD Degradations*: AiOIR models face significant difficulty in handling highly diverse and unforeseen image degradations, which can be treated as OOD degradations. In real-world scenarios, images may suffer from a combination of different degradations, such as blur, noise, low resolution, and compression artifacts. At the same time, the degree of each degradation type varies, and may be inconsistent with the sample distribution at training time while testing.

3) *Model Complexity and Efficiency*: Despite recent advancements in AiOIR, these models are often computationally expensive and complex. Their large size and high com-

putational demands make them impractical for deployment on resource-constrained devices such as mobile phones or embedded systems. Striking a balance between performance and efficiency remains a significant issue, requiring models to maintain high restoration quality without becoming too cumbersome.

4) *Limited High-Quality Real-world Data*: Many AiOIR models depend on large-scale, high-quality labeled datasets for supervised training, but acquiring these datasets is resource-intensive. Real-world degraded data is often scarce, and the unpredictability of degradations makes it difficult for models to perform well in practical applications.

5) *High Dimensional Data*: Current IR models primarily focus on 2D images, but handling 3D data and video sequences presents additional challenges. For video restoration, not only does each frame need high-quality restoration, but temporal consistency across frames must also be preserved. This adds complexity and demands more sophisticated methods that can integrate spatial and temporal information simultaneously.

B. Future Research Directions

Future research will focus on several key directions. First, establishing a robust multi-task learning theory will be essential to effectively address task conflicts and optimize information-sharing mechanisms. Second, reducing reliance on large-scale labeled datasets by exploring semi-supervised and unsupervised learning methods will improve the model's adaptability in data-scarce situations. Additionally, designing efficient models suitable for edge computing will make AiOIR more feasible for practical applications. Furthermore, investigating more complex real-world degradation scenarios will drive improvements in model performance across various environments. Finally, integrating large multimodal pretrained models and generative priors will enhance the restoration capabilities by leveraging rich multimodal data. These research directions will lay the foundation for the practicality and flexibility of AiOIR models, enabling them to tackle a broader range of real-world challenges.

1) *Incorporating Robust Multi-task Learning Theory*: The development of multi-task learning (MTL) theory for AiOIR is still in its early stages, presenting key research opportunities [57], [263]. Challenges include managing task conflicts, dynamically weighting tasks, and optimizing inter-task information sharing to avoid interference [126], [127]. Further improvements can come from determining optimal task sequences, prioritizing tasks based on degradation severity, and designing loss functions that balance conflicting objectives. Progress in these areas is essential for building efficient, generalizable AiOIR systems for real-world degradations.

2) *Robust Prompt Learning under Data Scarcity*: While prompt-based learning enhances adaptability in AiOIR, its tendency to overfit under limited or imbalanced training data is a key challenge. Future work may explore prompt-space regularization (e.g., sparsity or low-rank constraints) to limit over-specialization, as well as meta-learning frameworks (e.g., MAML) to promote generalization across unseen degradations. Incorporating degradation-aware conditioning can fur-

ther improve robustness. Overall, designing prompt mechanisms that generalize reliably remains an open and important direction.

3) Semi-Supervised and Unsupervised Learning Methods:

Reducing the dependency on large-scale labeled datasets is essential for the scalability and applicability of AiOIR models. Future research should focus on developing semi-supervised and unsupervised learning approaches that can learn effective representations from unlabeled or partially labeled data [264], [265]. Techniques such as self-supervised learning, contrastive learning, and unsupervised domain adaptation can be leveraged to improve model performance in scenarios where labeled data is scarce or unavailable. By advancing these methods, AiOIR models can become more adaptable to diverse and unforeseen degradations encountered in real-world conditions.

4) Platform-Aware Model Design and Efficient Approaches:

An important direction is developing edge-friendly AiOIR models that balance accuracy and efficiency for deployment on mobile and embedded devices [266], [267]. Techniques like compression, pruning, quantization, and architecture search help reduce resource use with minimal performance loss. In addition to these methods, more radical approaches such as binary neural networks (BNNs) and spiking neural networks (SNNs) offer promising avenues for AiOIR deployment. Recent works show their effectiveness in tasks like super-resolution and deraining [268]–[271]. Combined with lightweight transformers, edge-specific distillation, and early-exit strategies, these methods advance practical AiOIR deployment.

5) Addressing More Practical and Complex Degradations:

There is a need to focus on more practical tasks and datasets that reflect the complexities of real-world image degradations [28], [272]. Future research should explore composite and complex degradation scenarios, such as image restoration in nighttime conditions, deraining and dehazing in the dark, and images affected by multiple overlapping degradations rather than isolated, mixed single degradation tasks. Developing and utilizing datasets that capture these challenging conditions will enable models to learn from and be tested on data that closely resembles real-world challenges. This focus will drive the development of AiOIR models that are more robust and effective in practical applications.

6) Incorporating Large Multimodal Pretrained Models and Generative Priors:

Another promising avenue is exploiting large multimodal pretrained models, particularly those incorporating generative models, to enhance AiOIR tasks [273]–[276]. Models like CLIP [86] and recent advancements in generative models (e.g., stable diffusion [208]) have demonstrated remarkable abilities to capture complex data distributions across multiple modalities. By mining the rich representations and priors from these universal models, AiOIR can benefit from enhanced understanding of image content and context, leading to better restoration in low-level tasks.

7) Leveraging Multi-Modal Information:

Most current AiOIR models primarily rely on single-modal image information, such as RGB images, limiting their effectiveness in addressing complex restoration tasks. Future research can focus on integrating multi-modal information—like depth maps,

optical flow, and infrared images—into AiOIR frameworks [277]–[279]. This integration would provide models with rich contextual and structural insights, enhancing their ability to accurately recover images with varied degradations [280].

8) Establishment of Standardized Evaluation Protocols and Benchmarks: Unlike single image restoration tasks with established datasets, AiOIR lacks standardized benchmarks. To enable fair comparison, it's essential to develop unified evaluation protocols and diverse datasets covering real-world scenarios like high-resolution restoration, medical enhancement, old photo repair, and challenging weather conditions.

9) Extension to High-dimensional Data: In addition to RGB images, extending AiOIR methods to other data, such as video [281], [282], 3D data [282], [283], dynamic event data [284], [285], and hyperspectral data [286], presents significant opportunities for future research. Developing techniques that effectively integrate spatial, temporal, spectral, dynamic, and 3D information will be vital for applications such as video enhancement, 3D rendering, spectral analysis, and augmented reality. Addressing these challenges will expand the capabilities of AiOIR models, making them more versatile and applicable to a broader range of tasks.

10) Privacy Protection: AiOIR is increasingly deployed in medical imaging, surveillance, and autonomous driving, yet its ethical implications are seldom addressed. Prior work on machine unlearning [135] shows how to erase the influence of private data in AiOIR, suggesting future research can explore data deletion and privacy-preserving training. Beyond privacy, biased data or model priors can cause fairness issues like uneven performance or hallucinations. Furthermore, misuse risks must be considered, as restored content may be used maliciously in misinformation, surveillance overreach, or unauthorized identity synthesis. These issues highlight the need for responsible development and deployment.

VI. CONCLUSION

In this paper, we present a comprehensive review of recent advancements in all-in-one image restoration, a rapidly emerging domain that integrates multiple types of image degradations into a single framework. Through an in-depth exploration of state-of-the-art models, we emphasize their robust capabilities, diverse architectures, and the rigorous experiments. By contrasting these models with traditional single-task approaches, we underscore the limitations of the latter in addressing real-world complexities, while highlighting the significant gains in efficiency, adaptability, and scalability offered by AiOIR models.

Our comprehensive taxonomy of existing works offers a multi-dimensional perspective, covering structural innovations, key methodologies such as prompt learning, mixture-of-experts, the incorporation of multimodal models, and autonomous agents. We further present an analysis of critical datasets, providing researchers and practitioners with a holistic toolkit to better assess the current landscape of AiOIR. Despite the considerable strides made in recent years, challenges persist. Current models still struggle with handling complex and compounded degradations, lack computational efficiency, and

do not generalize well in real-world scenarios. We believe that future research will focus on several key areas: the development of more lightweight and efficient architectures, advancements in semi-supervised learning, and expanding the scope of AiOIR models to accommodate multimodal inputs and video data. Additionally, as the field progresses, innovations in cross-modal learning, real-time processing, and interpretability will likely become central to pushing the boundaries of what AiOIR systems can achieve.

In conclusion, AiOIR represents more than just a technical integration of multiple degradation types—it marks a paradigm shift toward unified, general-purpose vision models that can adapt to real-world complexity with minimal supervision. While significant progress has been made, substantial challenges remain, especially in scaling to real-world conditions, ensuring robustness under compounded degradations, and extending beyond visual-only inputs. We foresee future innovations at the intersection of efficient architecture design, multimodal representation learning, and autonomous adaptation mechanisms. By charting a comprehensive landscape of AiOIR, this review aims not only to inform but also to inspire a new wave of research that pushes the boundaries of what is possible in image restoration and beyond.

REFERENCES

- [1] A. Krizhevsky, I. Sutskever, and G. E. Hinton, “ImageNet classification with deep convolutional neural networks,” *Communications of the ACM*, vol. 60, no. 6, pp. 84–90, 2017.
- [2] A. Vaswani, N. Shazeer, N. Parmar, J. Uszkoreit, L. Jones, A. N. Gomez, Ł. Kaiser, and I. Polosukhin, “Attention is all you need,” in *NeurIPS*, vol. 30, 2017.
- [3] K. Dabov, A. Foi, V. Katkovnik, and K. Egiazarian, “Color image denoising via sparse 3d collaborative filtering with grouping constraint in luminance-chrominance space,” in *ICIP*, vol. 1. Ieee, 2007, pp. I–313.
- [4] J. Liu, J. Lin, X. Li, W. Zhou, S. Liu, and Z. Chen, “LIRA: Life-long image restoration from unknown blended distortions,” in *ECCV*. Springer, 2020, pp. 616–632.
- [5] C. Tian, Y. Xu, and W. Zuo, “Image denoising using deep cnn with batch renormalization,” *Neural Networks*, vol. 121, pp. 461–473, 2020.
- [6] K. Zhang, W. Zuo, Y. Chen, D. Meng, and L. Zhang, “Beyond a Gaussian Denoiser: Residual learning of deep cnn for image denoising,” *IEEE Trans. Image Process.*, vol. 26, no. 7, pp. 3142–3155, 2017.
- [7] K. Zhang, W. Zuo, S. Gu, and L. Zhang, “Learning deep cnn denoiser prior for image restoration,” in *CVPR*, 2017, pp. 3929–3938.
- [8] K. Zhang, W. Zuo, and L. Zhang, “FFDNet: Toward a fast and flexible solution for cnn-based image denoising,” *IEEE Trans. Image Process.*, vol. 27, no. 9, pp. 4608–4622, 2018.
- [9] B. Cai, X. Xu, K. Jia, C. Qing, and D. Tao, “DehazeNet: An end-to-end system for single image haze removal,” *IEEE Trans. Image Process.*, vol. 25, no. 11, pp. 5187–5198, 2016.
- [10] Y. Dong, Y. Liu, H. Zhang, S. Chen, and Y. Qiao, “FD-GAN: Generative adversarial networks with fusion-discriminator for single image dehazing,” in *AAAI*, vol. 34, no. 07, 2020, pp. 10 729–10 736.
- [11] X. Fan, Y. Wang, X. Tang, R. Gao, and Z. Luo, “Two-layer gaussian process regression with example selection for image dehazing,” *IEEE Trans. Circuits Syst. Video Technol.*, vol. 27, no. 12, pp. 2505–2517, 2016.
- [12] K. He, J. Sun, and X. Tang, “Single image haze removal using dark channel prior,” *IEEE Trans. Pattern Anal. Mach. Intell.*, vol. 33, no. 12, pp. 2341–2353, 2010.
- [13] B. Li, Y. Gou, S. Gu, J. Z. Liu, J. T. Zhou, and X. Peng, “You Only Look Yourself: Unsupervised and untrained single image dehazing neural network,” *Int. J. Comput. Vision*, vol. 129, pp. 1754–1767, 2021.
- [14] W.-T. Chen, H.-Y. Fang, C.-L. Hsieh, C.-C. Tsai, I. Chen, J.-J. Ding, S.-Y. Kuo *et al.*, “All Snow Removed: Single image desnowing algorithm using hierarchical dual-tree complex wavelet representation and contradict channel loss,” in *CVPR*, 2021, pp. 4196–4205.
- [15] S. Chen, T. Ye, C. Xue, H. Chen, Y. Liu, E. Chen, and L. Zhu, “Uncertainty-driven dynamic degradation perceiving and background modeling for efficient single image desnowing,” in *ACM MM*, 2023, pp. 4269–4280.
- [16] Y. Wang, C. Ma, and J. Liu, “Smartassign: Learning a smart knowledge assignment strategy for deraining and desnowing,” in *CVPR*, 2023, pp. 3677–3686.
- [17] D. Ren, W. Zuo, Q. Hu, P. Zhu, and D. Meng, “Progressive Image Deraining Networks: A better and simpler baseline,” in *CVPR*, 2019, pp. 3937–3946.
- [18] W. Yang, R. T. Tan, S. Wang, Y. Fang, and J. Liu, “Single Image Deraining: From model-based to data-driven and beyond,” *IEEE Trans. Pattern Anal. Mach. Intell.*, vol. 43, no. 11, pp. 4059–4077, 2020.
- [19] X. Chen, H. Li, M. Li, and J. shan Pan, “Learning a sparse transformer network for effective image deraining,” in *CVPR*, 2023, pp. 5896–5905.
- [20] X. Tao, H. Gao, X. Shen, J. Wang, and J. Jia, “Scale-recurrent network for deep image deblurring,” in *CVPR*, 2018, pp. 8174–8182.
- [21] L. Yuan, J. Sun, L. Quan, and H.-Y. Shum, “Image deblurring with blurred/noisy image pairs,” in *ACM SIGGRAPH*, 2007, pp. 1–es.
- [22] X. Guo, Y. Li, and H. Ling, “LIME: Low-light image enhancement via illumination map estimation,” *IEEE Trans. Image Process.*, vol. 26, no. 2, pp. 982–993, 2016.
- [23] L. Ma, T. Ma, R. Liu, X. Fan, and Z. Luo, “Toward fast, flexible, and robust low-light image enhancement,” in *CVPR*, 2022, pp. 5637–5646.
- [24] Y. Wang, W. Xie, and H. Liu, “Low-light image enhancement based on deep learning: a survey,” *Opt. Eng.*, vol. 61, no. 4, pp. 040 901–040 901, 2022.
- [25] X. Wang, L. Xie, C. Dong, and Y. Shan, “Real-ESRGAN: Training real-world blind super-resolution with pure synthetic data,” in *ICCV*, 2021, pp. 1905–1914.
- [26] Z. Yue, J. Wang, and C. C. Loy, “ResShift: Efficient diffusion model for image super-resolution by residual shifting,” *NeurIPS*, vol. 36, pp. 13 294–13 307, 2023.
- [27] J. Wang, Z. Yue, S. Zhou, K. C. Chan, and C. C. Loy, “Exploiting diffusion prior for real-world image super-resolution,” *IJCV*, 2024.
- [28] F. Yu, J. Gu, Z. Li, J. Hu, X. Kong, X. Wang, J. He, Y. Qiao, and C. Dong, “Scaling up to excellence: Practicing model scaling for photo-realistic image restoration in the wild,” in *CVPR*, 2024, pp. 25 669–25 680.
- [29] J. M. J. Valanarasu, R. Yasarla, and V. M. Patel, “TransWeather: Transformer-based restoration of images degraded by adverse weather conditions,” in *CVPR*, 2022, pp. 2353–2363.
- [30] H. Zhang, Y. Ba, E. Yang, V. Mehra, B. Gella, A. Suzuki, A. Pfahl, C. C. Chandrappa, A. Wong, and A. Kadambi, “WeatherStream: Light transport automation of single image dewatering,” in *CVPR*, 2023, pp. 13 499–13 509.
- [31] Y. Guo, Y. Gao, Y. Lu, H. Zhu, R. W. Liu, and S. He, “OneRestore: A universal restoration framework for composite degradation,” in *ECCV*, 2024, pp. 255–272.
- [32] L. Zhang, L. Zhang, and A. C. Bovik, “A feature-enriched completely blind image quality evaluator,” *IEEE Trans. Image Process.*, vol. 24, pp. 2579–2591, 2015.
- [33] H. R. Sheikh, A. C. Bovik, and G. De Veciana, “An information fidelity criterion for image quality assessment using natural scene statistics,” *IEEE Trans. Image Process.*, vol. 14, no. 12, pp. 2117–2128, 2005.
- [34] Z. Wang, J. Chen, and S. C. H. Hoi, “Deep learning for image super-resolution: A survey,” *IEEE Trans. Pattern Anal. Mach. Intell.*, vol. 43, no. 10, pp. 3365–3387, 2021.
- [35] S. Anwar, S. Khan, and N. Barnes, “A deep journey into super-resolution: A survey,” *ACM Compt. Surv.*, vol. 53, no. 3, pp. 1–34, 2020.
- [36] H. Chen, X. He, L. Qing, Y. Wu, C. Ren, R. E. Sheriff, and C. Zhu, “Real-world single image super-resolution: A brief review,” *Inf. Fus.*, vol. 79, pp. 124–145, 2022.
- [37] A. Liu, Y. Liu, J. Gu, Y. Qiao, and C. Dong, “Blind image super-resolution: A survey and beyond,” *IEEE Trans. Pattern Anal. Mach. Intell.*, vol. 45, no. 5, pp. 5461–5480, 2022.
- [38] H. Wang, Y. Wu, M. Li, Q. Zhao, and D. Meng, “Survey on rain removal from videos or a single image,” *Sci. China Inform. Sci.*, vol. 65, no. 1, pp. 1–23, 2022.
- [39] Z. Su, Y. Zhang, J. Shi, and X.-P. Zhang, “A survey of single image rain removal based on deep learning,” *ACM Compt. Surv.*, vol. 56, no. 4, pp. 1–35, 2023.
- [40] S. Krishna B V, B. Rajalakshmi, U. Dhammini, M. Monika, C. Nethra, and K. Ashok, “Image de-hazing techniques for vision based applications - a survey,” in *ICONAT*, 2023, pp. 1–5.

[41] C. Tian, L. Fei, W. Zheng, Y. Xu, W. Zuo, and C.-W. Lin, "Deep learning on image denoising: An overview," *Neural Networks*, vol. 131, pp. 251–275, 2020.

[42] B. Goyal, A. Dogra, S. Agrawal, B. S. Sohi, and A. Sharma, "Image denoising review: From classical to state-of-the-art approaches," *Inf. Fus.*, vol. 55, pp. 220–244, 2020.

[43] M. Elad, B. Kawar, and G. Vaksman, "Image denoising: The deep learning revolution and beyond—a survey paper," *SIAM J. Imaging Sci.*, vol. 16, no. 3, pp. 1594–1654, 2023.

[44] A. Mahalakshmi and B. Shanthini, "A survey on image deblurring," in *ICCCI*, 2016, pp. 1–5.

[45] A. Ranjan and R. M., "Deep learning based image deblurring: A comparative survey," in *ICAC3N*, 2022, pp. 996–1002.

[46] J. Liu, D. Xu, W. Yang, M. Fan, and H. Huang, "Benchmarking low-light image enhancement and beyond," *Int. J. Comput. Vision*, vol. 129, pp. 1153–1184, 2021.

[47] C. Li, C. Guo, L. Han, J. Jiang, M.-M. Cheng, J. Gu, and C. C. Loy, "Low-light image and video enhancement using deep learning: A survey," *IEEE Trans. Pattern Anal. Mach. Intell.*, vol. 44, no. 12, pp. 9396–9416, 2021.

[48] Y. Wang, R. Wan, W. Yang, H. Li, L.-P. Chau, and A. Kot, "Low-light image enhancement with normalizing flow," in *AAAI*, vol. 36, no. 3, 2022, pp. 2604–2612.

[49] X. Li, Y. Ren, X. Jin, C. Lan, X. K. Wang, W. Zeng, X. Wang, and Z. Chen, "Diffusion models for image restoration and enhancement - a comprehensive survey," *CoRR*, vol. abs/2308.09388, 2023.

[50] S. W. Zamir, A. Arora, S. H. Khan, M. Hayat, F. S. Khan, and M.-H. Yang, "Restormer: Efficient transformer for high-resolution image restoration," in *CVPR*, 2021, pp. 5718–5729.

[51] Z. Wang, X. Cun, J. Bao, W. Zhou, J. Liu, and H. Li, "Uformer: A general u-shaped transformer for image restoration," in *CVPR*, June 2022, pp. 17683–17693.

[52] L. Chen, X. Chu, X. Zhang, and J. Sun, "Simple baselines for image restoration," in *ECCV*, 2022.

[53] R. Li, R. T. Tan, and L. F. Cheong, "All in one bad weather removal using architectural search," in *CVPR*, 2020, pp. 3172–3182.

[54] B. Li, X. Liu, P. Hu, Z. Wu, J. Lv, and X. Peng, "All-in-one image restoration for unknown corruption," in *CVPR*, 2022, pp. 17452–17462.

[55] P. M. Uplavikar, Z. Wu, and Z. Wang, "All-in-one underwater image enhancement using domain-adversarial learning," in *CVPR workshops*, 2019, pp. 1–8.

[56] X. Zhang, H. Zhang, G. Wang, Q. Zhang, L. Zhang, and B. Du, "UniUIR: Considering underwater image restoration as an all-in-one learner," *arXiv preprint arXiv:2501.12981*, 2025.

[57] J. Zhang, J. Huang, M. Yao, Z. Yang, H. Yu, M. Zhou, and F. Zhao, "Ingredient-oriented multi-degradation learning for image restoration," in *CVPR*, 2023, pp. 5825–5835.

[58] V. Potlapalli, S. W. Zamir, S. H. Khan, and F. Shahbaz Khan, "Prompt-IR: Prompting for all-in-one image restoration," in *NeurIPS*, vol. 36, 2024.

[59] J. Ma, T. Cheng, G. Wang, Q. Zhang, X. Wang, and L. Zhang, "ProRes: Exploring degradation-aware visual prompt for universal image restoration," *arXiv preprint arXiv:2306.13653*, 2023.

[60] Y. Cheng, M. Shao, Y. Wan, and C. Wang, "RDM-IR: Task-adaptive deep unfolding network for all-in-one image restoration," *Knowledge-Based Systems*, vol. 304, p. 112543, 2024.

[61] Y. Jiang, Z. Zhang, T. Xue, and J. Gu, "AutoDIR: Automatic all-in-one image restoration with latent diffusion," in *ECCV*. Springer, 2024, pp. 340–359.

[62] M. Yao, R. Xu, Y. Guan, J. Huang, and Z. Xiong, "Neural degradation representation learning for all-in-one image restoration," *IEEE Trans. Image Process.*, vol. Pp, 2023.

[63] W.-T. Chen, Z.-K. Huang, C.-C. Tsai, H.-H. Yang, J.-J. Ding, and S.-Y. Kuo, "Learning multiple adverse weather removal via two-stage knowledge learning and multi-contrastive regularization: Toward a unified model," in *CVPR*, 2022, pp. 17632–17641.

[64] O. Özdenizci and R. Legenstein, "Restoring vision in adverse weather conditions with patch-based denoising diffusion models," *IEEE Trans. Pattern Anal. Mach. Intell.*, vol. 45, no. 8, pp. 10 346–10 357, 2023.

[65] Y. Zhu, T. Wang, X. Fu, X. Yang, X. Guo, J. Dai, Y. Qiao, and X. Hu, "Learning weather-general and weather-specific features for image restoration under multiple adverse weather conditions," in *CVPR*, 2023, pp. 21 747–21 758.

[66] T. Ye, S. Chen, J. Bai, J. Shi, C. Xue, J. Jiang, J. Yin, E. Chen, and Y. Liu, "Adverse weather removal with codebook priors," in *CVPR*, 2023, pp. 12 653–12 664.

[67] T. Wang, K. Zhang, Z. Shao, W. Luo, B. Stenger, T. Lu, T.-K. Kim, W. Liu, and H. Li, "GridFormer: Residual dense transformer with grid structure for image restoration in adverse weather conditions," *IJCV*, 2024.

[68] Y. Liu, Y. Xu, Y. Wei, X. Bi, and B. Xiao, "Clear Nights Ahead: Towards multi-weather nighttime image restoration," *arXiv preprint arXiv:2505.16479*, 2025.

[69] L. Yang, B. Kang, Z. Huang, Z. Zhao, X. Xu, J. Feng, and H. Zhao, "Depth anything v2," in *NeurIPS*, vol. 37, 2024, pp. 21 875–21 911.

[70] Z. Yang, H. Chen, Z. Qian, Y. Yi, H. Zhang, D. Zhao, B. Wei, and Y. Xu, "All-in-one medical image restoration via task-adaptive routing," in *MICCAI*. Springer, 2024, pp. 67–77.

[71] C. Ma, Z. Li, J. He, J. Zhang, Y. Zhang, and H. Shan, "Prompted contextual transformer for incomplete-view ct reconstruction," *arXiv preprint arXiv:2312.07846*, 2023.

[72] J. Zhang, D. Peng, C. Liu, P. Zhang, and L. Jin, "DocRes: A generalist model toward unifying document image restoration tasks," in *CVPR*, 2024, pp. 15 654–15 664.

[73] W. Lu, L. Su, J. Zheng, V. V. de Melo, F. Shoeeh, J. Hawkin, T. Tricco, H. Zhao, and X. Jiang, "TextDoctor: Unified document image inpainting via patch pyramid diffusion models," *Available at SSRN 5108776*, 2025.

[74] C.-M. Lee, C.-H. Cheng, Y.-F. Lin, Y.-C. Cheng, W.-T. Liao, C.-C. Hsu, F.-E. Yang, and Y.-C. F. Wang, "PromptHSI: Universal hyperspectral image restoration framework for composite degradation," *arXiv preprint arXiv:2411.15922*, 2024.

[75] Z. Wu, Y. Chen, N. Yokoya, and W. He, "MP-HSIR: A multi-prompt framework for universal hyperspectral image restoration," *arXiv preprint arXiv:2503.09131*, 2025.

[76] D. Feijoo, J. C. Benito, A. Garcia, and M. V. Conde, "DarkIR: Robust low-light image restoration," in *CVPR*, 2025.

[77] R. Schettini and S. Corchs, "Underwater image processing: state of the art of restoration and image enhancement methods," *EURASIP journal on advances in signal processing*, vol. 2010, pp. 1–14, 2010.

[78] H.-H. Wang, F.-J. Tsai, Y.-Y. Lin, and C.-W. Lin, "TANet: Triplet attention network for all-in-one adverse weather image restoration," in *ACCV*, 2024, pp. 835–851.

[79] Y. Cui, S. W. Zamir, S. Khan, A. Knoll, M. Shah, and F. S. Khan, "AdaIR: Adaptive all-in-one image restoration via frequency mining and modulation," in *ICLR*, 2025.

[80] J. Han, W. Li, P. Fang, C. Sun, J. Hong, M. A. Armin, L. Petersson, and H. Li, "Blind image decomposition," in *ECCV*. Springer, 2022, pp. 218–237.

[81] H. Chen, Y. Wang, T. Guo, C. Xu, Y. Deng, Z. Liu, S. Ma, C. Xu, C. Xu, and W. Gao, "Pre-trained image processing transformer," in *CVPR*, 2021, pp. 12 299–12 310.

[82] X. Yu, S. Zhou, H. Li, and L. Zhu, "Multi-Expert Adaptive Selection: Task-balancing for all-in-one image restoration," *CoRR*, vol. abs/2407.19139, 2024.

[83] X. Lin, J. Yue, K. C. Chan, L. Qi, C. Ren, J. Pan, and M.-H. Yang, "Multi-task image restoration guided by robust dino features," *arXiv preprint arXiv:2312.01677*, 2023.

[84] X. Zhang, J. Ma, G. Wang, Q. Zhang, H. Zhang, and L. Zhang, "Perceive-IR: Learning to perceive degradation better for all-in-one image restoration," *IEEE Trans. Image Process.*, 2025.

[85] Z. Luo, F. K. Gustafsson, Z. Zhao, J. Sjolund, and T. B. Schon, "Controlling vision-language models for multi-task image restoration," in *ICLR*, 2024.

[86] A. Radford, J. W. Kim, C. Hallacy, A. Ramesh, G. Goh, S. Agarwal, G. Sastry, A. Askell, P. Mishkin, J. Clark *et al.*, "Learning transferable visual models from natural language supervision," in *ICML*. Pmlr, 2021, pp. 8748–8763.

[87] M. Caron, H. Touvron, I. Misra, H. Jégou, J. Mairal, P. Bojanowski, and A. Joulin, "Emerging properties in self-supervised vision transformers," in *ICCV*, 2021, pp. 9630–9640.

[88] M. Oquab, T. Dariseti, T. Moutakanni, H. V. Vo, M. Szafraniec, V. Khaldov, P. Fernandez, D. Haziza, F. Massa, A. El-Nouby, M. Assran, N. Ballas, W. Galuba, R. Howes, P. Huang, S. Li, I. Misra, M. Rabbat, V. Sharma, G. Synnaeve, H. Xu, H. Jégou, J. Mairal, P. Labatut, A. Joulin, and P. Bojanowski, "Dinov2: Learning robust visual features without supervision," *Trans. Mach. Learn. Res.*, 2024.

[89] Z. Li, Y. Lei, C. Ma, J. Zhang, and H. Shan, "Prompt-in-prompt learning for universal image restoration," *arXiv*, 2023.

[90] D. Fan, J. Zhang, and L. Chang, "ConStyle v2: A strong prompter for all-in-one image restoration," *arXiv preprint arXiv:2406.18242*, 2024.

[91] Y. Zhang, H. Zhang, X. Chai, Z. Cheng, R. Xie, L. Song, and W. Zhang, “Diff-Restorer: Unleashing visual prompts for diffusion-based universal image restoration,” *arXiv preprint arXiv:2407.03636*, 2024.

[92] Z. Liu, S. Zhou, Y. Dai, Y. Wang, Y. An, and X. Zhao, “DPMambaIR: All-in-one image restoration via degradation-aware prompt state space model,” *arXiv preprint arXiv:2504.17732*, 2025.

[93] Q. Yan, A. Jiang, K. Chen, L. Peng, Q. Yi, and C. Zhang, “Textual prompt guided image restoration,” *Eng. Appl. Artif. Intell.*, vol. 155, p. 110981, 2025.

[94] M. V. Conde, G. Geigle, and R. Timofte, “High-quality image restoration following human instructions,” *arXiv preprint arXiv:2401.16468*, 2024.

[95] Y. Tian, J. Han, H. Chen, Y. Xi, G. Zhang, J. Hu, C. Xu, and Y. Wang, “Instruct- IPT: All-in-one image processing transformer via weight modulation,” *arXiv preprint arXiv:2407.00676*, 2024.

[96] Y. Liu, X. Chen, X. Ma, X. Wang, J. Zhou, Y. Qiao, and C. Dong, “Unifying image processing as visual prompting question answering,” *arXiv 2310.10513*, 2023.

[97] S. Chen, T. Ye, K. Zhang, Z. Xing, Y. Lin, and L. Zhu, “Teaching Tailored to Talent: Adverse weather restoration via prompt pool and depth-anything constraint,” in *ECCV*, 2024, pp. 95–115.

[98] L. Yang, B. Kang, Z. Huang, X. Xu, J. Feng, and H. Zhao, “Depth Anything: Unleashing the power of large-scale unlabeled data,” in *CVPR*, 2024.

[99] H. Yang, L. Pan, Y. Yang, and W. Liang, “Language-driven all-in-one adverse weather removal,” in *CVPR*, 2024, pp. 24902–24912.

[100] H. Duan, X. Min, S. Wu, W. Shen, and G. Zhai, “UniProcessor: a text-induced unified low-level image processor,” in *ECCV*. Springer, 2024, pp. 180–199.

[101] S. Ruder, M. E. Peters, S. Swayamdipta, and T. Wolf, “Transfer learning in natural language processing,” in *NAACL*, 2019, pp. 15–18.

[102] H. H. Mao, “A survey on self-supervised pre-training for sequential transfer learning in neural networks,” *arXiv preprint arXiv:2007.00800*, 2020.

[103] R. M. French, “Catastrophic forgetting in connectionist networks,” *Trends in Cognitive Sciences*, vol. 3, no. 4, pp. 128–135, 1999.

[104] X. Su, Z. Zheng, and C. Wu, “Review Learning: Advancing all-in-one ultra-high-definition image restoration training method,” *arXiv preprint arXiv:2408.06709*, 2024.

[105] X. Kong, C. Dong, and L. Zhang, “Towards effective multiple-in-one image restoration: A sequential and prompt learning strategy,” *arXiv preprint arXiv:2401.03379*, 2024.

[106] Z. Chen and B. Liu, *Lifelong machine learning*. Springer Nature, 2022.

[107] M. De Lange, R. Aljundi, M. Masana, S. Parisot, X. Jia, A. Leonardis, G. Slabaugh, and T. Tuytelaars, “A continual learning survey: Defying forgetting in classification tasks,” *IEEE Trans. Pattern Anal. Mach. Intell.*, vol. 44, no. 7, pp. 3366–3385, 2021.

[108] D. Mandal, S. Chattopadhyay, G. Tong, and P. Chakravarthula, “UniCoRN: Latent diffusion-based unified controllable image restoration network across multiple degradations,” *arXiv preprint arXiv:2503.15868*, 2025.

[109] T. Chen, S. Kornblith, M. Norouzi, and G. Hinton, “A simple framework for contrastive learning of visual representations,” in *ICML*. Pmlr, 2020, pp. 1597–1607.

[110] K. He, H. Fan, Y. Wu, S. Xie, and R. Girshick, “Momentum contrast for unsupervised visual representation learning,” in *CVPR*, 2020, pp. 9729–9738.

[111] G. Wu, J. Jiang, K. Jiang, and X. Liu, “Learning from history: Task-agnostic model contrastive learning for image restoration,” in *AAAI*, vol. 38, no. 6, Mar. 2024, pp. 5976–5984.

[112] H. Wu, Y. Qu, S. Lin, J. Zhou, R. Qiao, Z. Zhang, Y. Xie, and L. Ma, “Contrastive learning for compact single image dehazing,” in *CVPR*, 2021, pp. 10551–10560.

[113] G. Wu, J. Jiang, and X. Liu, “A practical contrastive learning framework for single-image super-resolution,” *IEEE Trans. Neural Netw. Learn. Syst.*, pp. 1–12, 2023.

[114] Y. Zheng, J. Zhan, S. He, J. Dong, and Y. Du, “Curricular contrastive regularization for physics-aware single image dehazing,” in *CVPR*, 2023, pp. 5785–5794.

[115] W. Ran, P. Ma, Z. He, H. Ren, and H. Lu, “Harnessing joint rain-/detail-aware representations to eliminate intricate rains,” in *ICLR*, 2024.

[116] G. Wu, J. Jiang, K. Jiang, X. Liu, and L. Nie, “Beyond Degradation Redundancy: Contrastive prompt learning for all-in-one image restoration,” *arXiv preprint arXiv:2504.09973*, 2025.

[117] H. Chung, B. Sim, D. Ryu, and J. C. Ye, “Improving diffusion models for inverse problems using manifold constraints,” in *NeurIPS*, 2022.

[118] H. Chung, J. Kim, M. T. McCann, M. L. Klasky, and J. C. Ye, “Diffusion posterior sampling for general noisy inverse problems,” *CoRR*, vol. abs/2209.14687, 2022.

[119] B. Fei, Z. Lyu, L. Pan, J. Zhang, W. Yang, T. Jian Luo, B. Zhang, and B. Dai, “Generative diffusion prior for unified image restoration and enhancement,” in *CVPR*, 2023, pp. 9935–9946.

[120] B. Kawar, M. Elad, S. Ermon, and J. Song, “Denoising diffusion restoration models,” in *NeurIPS*, 2022.

[121] Y. Ai, H. Huang, X. Zhou, J. Wang, and R. He, “Multimodal prompt perceiver: Empower adaptiveness generalizability and fidelity for all-in-one image restoration,” in *CVPR*, 2024, pp. 25432–25444.

[122] Y. Gou, H. Zhao, B. Li, X. Xiao, and X. Peng, “Test-time degradation adaptation for open-set image restoration,” in *ICML*, 2023.

[123] I. Shin, Y.-H. Tsai, B. Zhuang, S. Schulter, B. Liu, S. Garg, I.-S. Kweon, and K.-J. Yoon, “MM-TTA: Multi-modal test-time adaptation for 3d semantic segmentation,” in *CVPR*, 2022, pp. 16907–16916.

[124] Q. Wang, O. Fink, L. V. Gool, and D. Dai, “Continual test-time domain adaptation,” in *CVPR*, 2022, pp. 7191–7201.

[125] S. Niu, J. Wu, Y. Zhang, Z. Wen, Y. Chen, P. Zhao, and M. Tan, “Towards stable test-time adaptation in dynamic wild world,” *CoRR*, vol. abs/2302.12400, 2023.

[126] T. Yu, S. Kumar, A. Gupta, S. Levine, K. Hausman, and C. Finn, “Gradient surgery for multi-task learning,” in *NeurIPS*, 2020, pp. 5824–5836.

[127] B. Liu, X. Liu, X. Jin, P. Stone, and Q. Liu, “Conflict-averse gradient descent for multi-task learning,” in *NeurIPS*, 2021.

[128] C. Fifty, E. Amid, Z. Zhao, T. Yu, R. Anil, and C. Finn, “Efficiently identifying task groupings for multi-task learning,” in *NeurIPS*, vol. 34, 2021, pp. 27503–27516.

[129] S. Cao, Y. Liu, W. Zhang, Y. Qiao, and C. Dong, “GRIDS: Grouped multiple-degradation restoration with image degradation similarity,” in *ECCV*. Springer, 2024, pp. 70–87.

[130] G. Wu, J. Jiang, K. Jiang, and X. Liu, “Harmony in Diversity: Improving all-in-one image restoration via multi-task collaboration,” in *ACM MM*, 2024.

[131] G. Wu, J. Jiang, Y. Wang, K. Jiang, and X. Liu, “Debiased all-in-one image restoration with task uncertainty regularization,” in *AAAI*, vol. 39, no. 8, 2025, pp. 8386–8394.

[132] Y. Cao and J. Yang, “Towards making systems forget with machine unlearning,” *ISSP*, pp. 463–480, 2015.

[133] L. Bourtoule, V. Chandrasekaran, C. A. Choquette-Choo, H. Jia, A. Travers, B. Zhang, D. Lie, and N. Papernot, “Machine unlearning,” *ISSP*, pp. 141–159, 2019.

[134] Q. P. Nguyen, B. K. H. Low, and P. Jaillet, “Variational bayesian unlearning,” in *NeurIPS*, 2020.

[135] X. Su and Z. Zheng, “Accurate forgetting for all-in-one image restoration model,” *arXiv preprint arXiv:2409.00685*, 2024.

[136] T. Brown, B. Mann, N. Ryder, M. Subbiah, J. D. Kaplan, P. Dhariwal, A. Neelakantan, P. Shyam, G. Sastry, A. Askell *et al.*, “Language models are few-shot learners,” in *NeurIPS*, vol. 33, 2020, pp. 1877–1901.

[137] T. Gao, A. Fisch, and D. Chen, “Making pre-trained language models better few-shot learners,” *arXiv*, 2020.

[138] X. Liu, K. Ji, Y. Fu, W. L. Tam, Z. Du, Z. Yang, and J. Tang, “P-Tuning v2: Prompt tuning can be comparable to fine-tuning universally across scales and tasks,” *arXiv*, 2021.

[139] M. Jia, L. Tang, B.-C. Chen, C. Cardie, S. Belongie, B. Hariharan, and S.-N. Lim, “Visual prompt tuning,” in *ECCV*. Springer, 2022, pp. 709–727.

[140] M. U. Khattak, H. Rasheed, M. Maaz, S. Khan, and F. S. Khan, “MaPLE: Multi-modal prompt learning,” in *CVPR*, 2023, pp. 19113–19122.

[141] A. Bar, Y. Gandomi, T. Darrell, A. Globerson, and A. Efros, “Visual prompting via image inpainting,” in *NeurIPS*, vol. 35, 2022, pp. 25005–25017.

[142] T. Chen, S. Saxena, L. Li, T.-Y. Lin, D. J. Fleet, and G. E. Hinton, “A unified sequence interface for vision tasks,” in *NeurIPS*, vol. 35, 2022, pp. 31333–31346.

[143] Y. Wen, T. Gao, J. Zhang, Z. Li, and T. Chen, “Multi-axis prompt and multi-dimension fusion network for all-in-one weather-degraded image restoration,” in *AAAI*, vol. 39, no. 8, 2025, pp. 8323–8331.

[144] K. He, X. Chen, S. Xie, Y. Li, P. Doll’ar, and R. B. Girshick, “Masked autoencoders are scalable vision learners,” in *CVPR*, 2021, pp. 15979–15988.

[145] G. Wu, J. Jiang, K. Jiang, X. Liu, and L. Nie, “Learning dynamic prompts for all-in-one image restoration,” *IEEE Trans. Image Process.*, 2025.

[146] Y. Pang, Y. Li, J. Shen, and L. Shao, "Towards bridging semantic gap to improve semantic segmentation," in *ICCV*, 2019, pp. 4229–4238.

[147] Y. Wei, Z. Zhang, J. Ren, X. Xu, R. Hong, Y. Yang, S. Yan, and M. Wang, "Clarity ChatGPT: An interactive and adaptive processing system for image restoration and enhancement," *arXiv preprint arXiv:2311.11695*, 2023.

[148] R. Liao, F. Li, Y. Wei, Z. Shi, L. Zhang, H. Bai, and M. Wang, "Prompt to Restore, Restore to Prompt: Cyclic prompting for universal adverse weather removal," *arXiv preprint arXiv:2503.09013*, 2025.

[149] H. Zeng, X. Wang, Y. Chen, J. Su, and J. Liu, "Vision-language gradient descent-driven all-in-one deep unfolding networks," in *CVPR*, 2025.

[150] R. A. Jacobs, M. I. Jordan, S. J. Nowlan, and G. E. Hinton, "Adaptive mixtures of local experts," *Neural Computation*, vol. 3, no. 1, pp. 79–87, 1991.

[151] Y. Luo, R. Zhao, X. Wei, J. Chen, Y. Lu, S. Xie, T. Wang, R. Xiong, M. Lu, and S. Zhang, "WM-MoE: Weather-aware multi-scale mixture-of-experts for blind adverse weather removal," *arXiv preprint arXiv:2303.13739*, 2023.

[152] R. Zhang, Y. Luo, J. Liu, H. Yang, Z. Dong, D. Gudovskiy, T. Okuno, Y. Nakata, K. Keutzer, Y. Du *et al.*, "Efficient deweather mixture-of-experts with uncertainty-aware feature-wise linear modulation," in *AAAI*, vol. 38, no. 15, 2024, pp. 16812–16820.

[153] E. Zamfir, Z. Wu, N. Mehta, Y. Tan, D. P. Paudel, Y. Zhang, and R. Timofte, "Complexity experts are task-discriminative learners for any image restoration," in *CVPR*, 2025.

[154] J. Lin, Z. Zhang, W. Li, R. Pei, H. Xu, H. Zhang, and W. Zuo, "UniRestorer: Universal image restoration via adaptively estimating image degradation at proper granularity," *arXiv preprint arXiv:2412.20157*, 2024.

[155] Y. Ai, H. Huang, and R. H. Lora-ir, "Taming low-rank experts for efficient all-in-one image restoration," *arXiv preprint arXiv:2410.15385*, 2024.

[156] Y. Pu, L. Zhuo, K. Zhu, L. Xie, W. Zhang, X. Chen, P. Gao, Y. Qiao, C. Dong, and Y. Liu, "Lumina-OmniLV: A unified multimodal framework for general low-level vision," *arXiv preprint arXiv:2504.04903*, 2025.

[157] V. Frants, S. Agaian, K. Panetta, and P. Huang, "CMAWRNet: Multiple adverse weather removal via a unified quaternion neural architecture," *arXiv preprint arXiv:2505.01882*, 2025.

[158] K. Zhu, J. Gu, Z. You, Y. Qiao, and C. Dong, "An intelligent agentic system for complex image restoration problems," in *ICLR*, 2025.

[159] Y. Zhou, J. Cao, Z. Zhang, F. Wen, Y. Jiang, J. Jia, X. Liu, X. Min, and G. Zhai, "Q-Agent: Quality-driven chain-of-thought image restoration agent through robust multimodal large language model," *arXiv preprint arXiv:2504.07148*, 2025.

[160] H. Chen, W. Li, J. Gu, J. Ren, S. Chen, T. Ye, R. Pei, K. Zhou, F. Song, and L. Zhu, "RestoreAgent: Autonomous image restoration agent via multimodal large language models," in *NeurIPS*, 2024.

[161] J. Cao, D. Meng, and X. Cao, "Chain-of-Restoration: Multi-task image restoration models are zero-shot step-by-step universal image restorers," *arXiv preprint arXiv:2410.08688*, 2024.

[162] X. Jiang, G. Li, B. Chen, and J. Zhang, "Multi-agent image restoration," *arXiv preprint arXiv:2503.09403*, 2025.

[163] B. Li, X. Li, Y. Lu, and Z. Chen, "Hybrid agents for image restoration," *arXiv preprint arXiv:2503.10120*, 2025.

[164] K. Zhang, W. Zuo, S. Gu, and L. Zhang, "Learning deep cnn denoiser prior for image restoration," in *CVPR*, 2017, pp. 2808–2817.

[165] D. Geman and C. Yang, "Nonlinear image recovery with half-quadratic regularization," *IEEE Trans. Image Process.*, vol. 4, 7, pp. 932–946, 1995.

[166] M. Liu, W. Yang, J. Luo, and J. Liu, "UP-Restorer: When unrolling meets prompts for unified image restoration," in *AAAI*, vol. 39, no. 5, 2025, pp. 5513–5522.

[167] S. Nah, T. Hyun Kim, and K. Mu Lee, "Deep multi-scale convolutional neural network for dynamic scene deblurring," in *CVPR*, 2017, pp. 3883–3891.

[168] Z. Shen, W. Wang, X. Lu, J. Shen, H. Ling, T. Xu, and L. Shao, "Human-aware motion deblurring," in *CVPR*, 2019, pp. 5572–5581.

[169] J. Rim, H. Lee, J. Won, and S. Cho, "Real-world blur dataset for learning and benchmarking deblurring algorithms," in *ECCV*. Springer, 2020, pp. 184–201.

[170] R. Franzen, "Kodak lossless true color image suite," *Source: https://r0k.us/graphics/kodak/*, 1999.

[171] J.-B. Huang, A. Singh, and N. Ahuja, "Single image super-resolution from transformed self-exemplars," in *CVPR*, 2015, pp. 5197–5206.

[172] K. Ma, Z. Duanmu, Q. Wu, Z. Wang, H. Yong, H. Li, and L. Zhang, "Waterloo Exploration Database: New challenges for image quality assessment models," *IEEE Trans. Image Process.*, vol. 26, no. 2, pp. 1004–1016, 2016.

[173] P. Arbelaez, M. Maire, C. Fowlkes, and J. Malik, "Contour detection and hierarchical image segmentation," *IEEE Trans. Pattern Anal. Mach. Intell.*, vol. 33, no. 5, pp. 898–916, 2010.

[174] D. Martin, C. Fowlkes, D. Tal, and J. Malik, "A database of human segmented natural images and its application to evaluating segmentation algorithms and measuring ecological statistics," in *ICCV*, vol. 2. Ieee, 2001, pp. 416–423.

[175] L. Zhang, X. Wu, A. Buades, and X. Li, "Color demosaicking by local directional interpolation and nonlocal adaptive thresholding," *J Electron Imaging*, vol. 20, no. 2, pp. 023016–023016, 2011.

[176] E. Agustsson and R. Timofte, "Ntire 2017 challenge on single image super-resolution: Dataset and study," in *CVPR*, Jul. 2017.

[177] Y. Wang, L. Wang, J. Yang, W. An, and Y. Guo, "Flickr1024: A large-scale dataset for stereo image super-resolution," in *ICCVW*, 2019.

[178] M. Bevilacqua, A. Roumy, C. M. Guillemot, and M.-L. Alberi-Morel, "Low-complexity single-image super-resolution based on nonnegative neighbor embedding," in *BMVC*, 2012.

[179] R. Zeyde, M. Elad, and M. Protter, "On single image scale-up using sparse-representations," in *ICCS*. Springer, 2012, pp. 711–730.

[180] J. Wang, X. Li, and J. Yang, "Stacked conditional generative adversarial networks for jointly learning shadow detection and shadow removal," in *CVPR*, 2018, pp. 1788–1797.

[181] L. Qu, J. Tian, S. He, Y. Tang, and R. W. Lau, "DeshadowNet: A multi-context embedding deep network for shadow removal," in *CVPR*, 2017, pp. 4067–4075.

[182] Y.-F. Liu, D.-W. Jaw, S.-C. Huang, and J.-N. Hwang, "DesnowNet: Context-aware deep network for snow removal," *IEEE Trans. Image Process.*, vol. 27, no. 6, pp. 3064–3073, 2018.

[183] X. Zhang, H. Dong, J. Pan, C. Zhu, Y. Tai, C. Wang, J. Li, F. Huang, and F. Wang, "Learning to restore hazy video: A new real-world dataset and a new method," in *CVPR*, 2021, pp. 9239–9248.

[184] J. Wang, C. Lin, L. Nie, S. Huang, Y. Zhao, X. Pan, and R. Ai, "WeatherDepth: Curriculum contrastive learning for self-supervised depth estimation under adverse weather conditions," in *ICRA*. IEEE, 2024, pp. 4976–4982.

[185] R. Qian, R. T. Tan, W. Yang, J. Su, and J. Liu, "Attentive generative adversarial network for raindrop removal from a single image," in *CVPR*, 2018, pp. 2482–2491.

[186] R. Li, L.-F. Cheong, and R. T. Tan, "Heavy Rain Image Restoration: Integrating physics model and conditional adversarial learning," in *CVPR*, 2019, pp. 1633–1642.

[187] T. Wang, X. Yang, K. Xu, S. Chen, Q. Zhang, and R. W. Lau, "Spatial attentive single-image deraining with a high quality real rain dataset," in *CVPR*, 2019, pp. 12270–12279.

[188] X. Fu, J. Huang, D. Zeng, Y. Huang, X. Ding, and J. Paisley, "Removing rain from single images via a deep detail network," in *CVPR*, 2017, pp. 3855–3863.

[189] W. Yang, R. T. Tan, J. Feng, J. Liu, Z. Guo, and S. Yan, "Deep joint rain detection and removal from a single image," in *CVPR*, 2017, pp. 1357–1366.

[190] C. O. Ancuti, C. Ancuti, M. Sbert, and R. Timofte, "Dense-Haze: A benchmark for image dehazing with dense-haze and haze-free images," in *ICIP*. Ieee, 2019, pp. 1014–1018.

[191] B. Li, W. Ren, D. Fu, D. Tao, D. Feng, W. Zeng, and Z. Wang, "Benchmarking single-image dehazing and beyond," *IEEE Trans. Image Process.*, vol. 28, no. 1, pp. 492–505, 2019.

[192] C. Wei, W. Wang, W. Yang, and J. Liu, "Deep retinex decomposition for low-light enhancement," in *BMVC*, 2018.

[193] C. Jia, Y. Yang, Y. Xia, Y.-T. Chen, Z. Parekh, H. Pham, Q. V. Le, Y.-H. Sung, Z. Li, and T. Duerig, "Scaling up visual and vision-language representation learning with noisy text supervision," in *ICML*, 2021.

[194] J. Li, D. Li, C. Xiong, and S. C. H. Hoi, "BLIP: Bootstrapping language-image pre-training for unified vision-language understanding and generation," in *ICML*, 2022.

[195] M. Shao, Y. Liu, Y. Cheng, Y. Wan, and C. Wang, "Adaptive fuzzy degradation perception based on clip prior for all-in-one image restoration," *IEEE Trans. Fuzzy Syst.*, 2024.

[196] S. Rajagopalan and V. M. Patel, "AWRaCLE: All-weather image restoration using visual in-context learning," in *AAAI*, vol. 39, no. 6, 2025, pp. 6675–6683.

[197] Z. Xie, Z. Zhang, Y. Cao, Y. Lin, J. Bao, Z. Yao, Q. Dai, and H. Hu, "SimMIM: a simple framework for masked image modeling," in *CVPR*, 2021, pp. 9643–9653.

[198] X. Wang, W. Wang, Y. Cao, C. Shen, and T. Huang, “Images Speak in Images: A generalist painter for in-context visual learning,” in *CVPR*, 2022, pp. 6830–6839.

[199] A. Radford and K. Narasimhan, “Improving language understanding by generative pre-training,” *OpenAI Blog*, 2018.

[200] J. Devlin, M.-W. Chang, K. Lee, and K. Toutanova, “BERT: Pre-training of deep bidirectional transformers for language understanding,” in *NAACL*, 2019.

[201] C.-J. Qin, R.-Q. Wu, Z. Liu, X. Lin, C.-L. Guo, H. H. Park, and C. Li, “Restore Anything with Masks: Leveraging mask image modeling for blind all-in-one image restoration,” in *ECCV*. Springer, 2024, pp. 364–380.

[202] A. Dudhane, O. Thawakar, S. W. Zamir, S. Khan, F. S. Khan, and M.-H. Yang, “Dynamic Pre-training: Towards efficient and scalable all-in-one image restoration,” *CoRR*, vol. abs/2404.02154, 2024.

[203] J. Jiang, T. Ding, K. Zhang, J. Zhou, T. Chen, I. Zharkov, Z. Zhu, and L. Liang, “Cat-AIR: Content and task-aware all-in-one image restoration,” *arXiv preprint arXiv:2503.17915*, 2025.

[204] D. Ha, A. Dai, and Q. V. Le, “Hypernetworks,” *arXiv preprint arXiv:1609.09106*, 2016.

[205] J. Cao, Y. Cao, L. Pang, D. Meng, and X. Cao, “HAIR: Hypernetworks-based all-in-one image restoration,” *CoRR*, vol. abs/2408.08091, 2024.

[206] R. Zhu, Z. Tu, J. Liu, A. C. Bovik, and Y. Fan, “MWFormer: Multi-weather image restoration using degradation-aware transformers,” *IEEE Trans. Image Process.*, 2024.

[207] K. Tian, Y. Jiang, Z. Yuan, B. Peng, and L. Wang, “Visual autoregressive modeling: Scalable image generation via next-scale prediction,” in *NeurIPS*, vol. 37, 2024, pp. 84 839–84 865.

[208] R. Rombach, A. Blattmann, D. Lorenz, P. Esser, and B. Ommer, “High-resolution image synthesis with latent diffusion models,” in *CVPR*, 2022, pp. 10 684–10 695.

[209] S. Wang and F. Zhao, “Varformer: Adapting var’s generative prior for image restoration,” *arXiv preprint arXiv:2412.21063*, 2024.

[210] S. Rajagopalan, K. Narayan, and V. M. Patel, “RestoreVAR: Visual autoregressive generation for all-in-one image restoration,” 2025.

[211] H. Li, X. Chen, J. Dong, J. Tang, and J. Pan, “FoundIR: Unleashing million-scale training data to advance foundation models for image restoration,” *arXiv preprint arXiv:2412.01427*, 2024.

[212] Z. Wang, A. C. Bovik, H. R. Sheikh, and E. P. Simoncelli, “Image Quality Assessment: from error visibility to structural similarity,” *IEEE Trans. Image Process.*, vol. 13, pp. 600–612, 2004.

[213] M. Heusel, H. Ramsauer, T. Unterthiner, B. Nessler, and S. Hochreiter, “GANs trained by a two time-scale update rule converge to a local nash equilibrium,” in *NeurIPS*, vol. 30, 2017.

[214] R. Zhang, P. Isola, A. A. Efros, E. Shechtman, and O. Wang, “The unreasonable effectiveness of deep features as a perceptual metric,” in *CVPR*, 2018, pp. 586–595.

[215] A. Mittal, R. Soundararajan, and A. C. Bovik, “Making a “completely blind” image quality analyzer,” *IEEE Signal Proc. Let.*, vol. 20, no. 3, pp. 209–212, 2012.

[216] A. Mittal, A. K. Moorthy, and A. C. Bovik, “No-reference image quality assessment in the spatial domain,” *IEEE Trans. Image Process.*, vol. 21, pp. 4695–4708, 2012.

[217] H. Talebi and P. Milanfar, “NIMA: Neural image assessment,” *IEEE Trans. Image Process.*, vol. 27, no. 8, pp. 3998–4011, 2018.

[218] J. Wang, K. C. K. Chan, and C. C. Loy, “Exploring clip for assessing the look and feel of images,” in *AAAI*, 2022.

[219] S. Wang, J. Zheng, H.-M. Hu, and B. Li, “Naturalness preserved enhancement algorithm for non-uniform illumination images,” *IEEE Trans. Image Process.*, vol. 22, no. 9, pp. 3538–3548, 2013.

[220] C. Saharia, J. Ho, W. Chan, T. Salimans, D. J. Fleet, and M. Norouzi, “Image super-resolution via iterative refinement,” *IEEE Trans. Pattern Anal. Mach. Intell.*, vol. 45, no. 4, pp. 4713–4726, 2023.

[221] J. Ke, Q. Wang, Y. Wang, P. Milanfar, and F. Yang, “MUSIQ: Multi-scale image quality transformer,” in *ICCV*, 2021, pp. 5128–5137.

[222] H. Gao, X. Tao, X. Shen, and J. Jia, “Dynamic scene deblurring with parameter selective sharing and nested skip connections,” in *CVPR*, 2019, pp. 3843–3851.

[223] H. Shen, Z.-Q. Zhao, and W. Zhang, “Adaptive dynamic filtering network for image denoising,” in *AAAI*, vol. 37, no. 2, 2023, pp. 2227–2235.

[224] Y. Song, Z. He, H. Qian, and X. Du, “Vision transformers for single image dehazing,” *IEEE Trans. Image Process.*, vol. 32, pp. 1927–1941, 2022.

[225] S. W. Zamir, A. Arora, S. H. Khan, M. Hayat, F. S. Khan, M.-H. Yang, and L. Shao, “Multi-stage progressive image restoration,” in *CVPR*, 2021, pp. 14 816–14 826.

[226] Y. Cui, W. Ren, X. Cao, and A. Knoll, “Image restoration via frequency selection,” *IEEE Trans. Pattern Anal. Mach. Intell.*, vol. 46, pp. 1093–1108, 2023.

[227] H. Guo, J. Li, T. Dai, Z. Ouyang, X. Ren, and S.-T. Xia, “MambaIR: A simple baseline for image restoration with state-space model,” in *ECCV*, 2024.

[228] Q. Fan, D. Chen, L. Yuan, G. Hua, N. Yu, and B. Chen, “A general decoupled learning framework for parameterized image operators,” *IEEE Trans. Pattern Anal. Mach. Intell.*, vol. 43, no. 1, pp. 33–47, 2019.

[229] B. Ren, E. Zamfir, Y. Li, Z. Wu, D. P. Paudel, R. Timofte, N. Sebe, and L. V. Gool, “Any image restoration with efficient automatic degradation adaptation,” *CoRR*, vol. abs/2407.13372, 2024.

[230] E. Zamfir, Z. Wu, N. Mehta, D. D. Paudel, Y. Zhang, and R. Timofte, “Efficient degradation-aware any image restoration,” *CoRR*, vol. abs/2405.15475, 2024.

[231] Y. Xu, N. Gao, Z. Shan, F. Chao, and R. Ji, “Unified-width adaptive dynamic network for all-in-one image restoration,” *CoRR*, vol. abs/2401.13221, 2024.

[232] Z. Shi, T. Su, P. Liu, Y. Wu, L. Zhang, and M. Wang, “Learning frequency-aware dynamic transformers for all-in-one image restoration,” *CoRR*, vol. abs/2407.01636, 2024.

[233] X. Tang, X. Gu, X. He, X. Hu, and J. Sun, “Degradation-aware residual-conditioned optimal transport for unified image restoration,” *IEEE Trans. Pattern Anal. Mach. Intell.*, 2025.

[234] D. Serrano-Lozano, L. Herranz, S. Su, and J. Vazquez-Corral, “Adaptive blind all-in-one image restoration,” *arXiv preprint arXiv:2411.18412*, 2024.

[235] A. Jiang, H. Chen, Z. Chen, J. Ye, and M. Wang, “Multi-dimensional visual prompt enhanced image restoration via mamba-transformer aggregation,” *arXiv preprint arXiv:2412.15845*, 2024.

[236] H. JiaKui, Z. Yao, J. Lujia, and L. Yanye, “Universal image restoration pre-training via degradation classification,” in *ICLR*, 2025.

[237] A. Tang, Y. Wu, and Y. Zhang, “RamIR: Reasoning and action prompting with mamba for all-in-one image restoration,” *Applied Intelligence*, vol. 55, no. 4, p. 258, 2025.

[238] G. Wu, J. Jiang, K. Jiang, and X. Liu, “Content-aware transformer for all-in-one image restoration,” *arXiv preprint arXiv:2504.04869*, 2025.

[239] B. Ren, E. Zamfir, Z. Wu, Y. Li, Y. Li, D. P. Paudel, R. Timofte, M.-H. Yang, L. Van Gool, and N. Sebe, “Any image restoration via efficient spatial-frequency degradation adaptation,” *arXiv preprint arXiv:2504.14249*, 2025.

[240] B. Ren, Y. Li, X. Zheng, Y. Fu, D. P. Paudel, M.-H. Yang, L. Van Gool, and N. Sebe, “Manifold-aware representation learning for degradation-agnostic image restoration,” *arXiv preprint arXiv:2505.18679*, 2025.

[241] X. Tang, X. He, X. Gu, and J. Sun, “BarylR: Learning multi-source unified representation in continuous barycenter space for generalizable all-in-one image restoration,” *arXiv preprint arXiv:2505.21637*, 2025.

[242] G. Wu, J. Jiang, K. Jiang, and X. Liu, “Boosting all-in-one image restoration via self-improved privilege learning,” 2025.

[243] X. Tian, X. Liao, X. Liu, M. Li, and C. Ren, “Degradation-aware feature perturbation for all-in-one image restoration,” in *CVPR*, 2025.

[244] H. Wang, M. Song, and G. Zhong, “Dynamic degradation decomposition network for all-in-one image restoration,” *arXiv preprint arXiv:2502.19068*, 2025.

[245] L. Liu, L. Xie, X. Zhang, S. Yuan, X. Chen, W. Zhou, H. Li, and Q. Tian, “TAPE: Task-agnostic prior embedding for image restoration,” in *ECCV*. Springer, 2022, pp. 447–464.

[246] Z. Chen, Y. Zhang, L. Ding, X. Bin, J. Gu, L. Kong, and X. Yuan, “Hierarchical integration diffusion model for realistic image deblurring,” in *NeurIPS*, 2023.

[247] Y. Cai, H. Bian, J. Lin, H. Wang, R. Timofte, and Y. Zhang, “RetinexFormer: One-stage retinex-based transformer for low-light image enhancement,” in *ICCV*, 2023.

[248] Z. Liu, Y. Lin, Y. Cao, H. Hu, Y. Wei, Z. Zhang, S. Lin, and B. Guo, “Swin Transformer: Hierarchical vision transformer using shifted windows,” in *ICCV*, 2021, pp. 9992–10 002.

[249] S. W. Zamir, A. Arora, S. Khan, M. Hayat, F. S. Khan, M.-H. Yang, and L. Shao, “Learning enriched features for fast image restoration and enhancement,” *IEEE Trans. Pattern Anal. Mach. Intell.*, 2022.

[250] C. Mou, Q. Wang, and J. Zhang, “Deep generalized unfolding networks for image restoration,” in *CVPR*, 2022.

[251] J. Zhang, J. Huang, M. Zhou, C. Li, and F. Zhao, “Decomposition ascribed synergistic learning for unified image restoration,” *CoRR*, vol. abs/2308.00759, 2023.

[252] Y.-W. Chen and S.-C. Pei, “Always clear days: Degradation type and severity aware all-in-one adverse weather removal,” *IEEE Access*, 2025.

[253] S. Sun, W. Ren, X. Gao, R. Wang, and X. Cao, "Restoring images in adverse weather conditions via histogram transformer," in *ECCV*, 2024, pp. 111–129.

[254] J. Xiong, X. Yan, Y. Wang, W. Zhao, X.-P. Zhang, and M. Wei, "DA2Diff: Exploring degradation-aware adaptive diffusion priors for all-in-one weather restoration," *arXiv preprint arXiv:2504.05135*, 2025.

[255] J. Wu, Z. Yang, Z. Wang, and Z. Jin, "Beyond Degradation Conditions: All-in-one image restoration via hog transformers," *arXiv preprint arXiv:2504.09377*, 2025.

[256] H. Wang, Q. Hu, and X. Guo, "MODEM: A morton-order degradation estimation mechanism for adverse weather image recovery," 2025.

[257] J. Mao, Y. Yang, X. Yin, L. Shao, and H. Tang, "AllRestorer: All-in-one transformer for image restoration under composite degradations," *arXiv preprint arXiv:2411.10708*, 2024.

[258] Y. Li, Y. Fan, X. Xiang, D. Demandolx, R. Ranjan, R. Timofte, and L. V. Gool, "Efficient and explicit modelling of image hierarchies for image restoration," in *CVPR*, 2023, pp. 18 278–18 289.

[259] B. Song, X. Chen, S. Xu, and J. Zhou, "Under-display camera image restoration with scattering effect," in *ICCV*, 2023, pp. 12 580–12 589.

[260] M. Zhou, J. Huang, C.-L. Guo, and C. Li, "Fourmer: An efficient global modeling paradigm for image restoration," in *ICML*, 2023, pp. 42 589–42 601.

[261] Y. Cui, W. Ren, and A. Knoll, "Omni-kernel network for image restoration," in *AAAI*, 2024, pp. 1426–1434.

[262] Z. Liu, Y. Lu, H. Yu *et al.*, "VL-UR: Vision-language-guided universal restoration of images degraded by adverse weather conditions," *arXiv preprint arXiv:2504.08219*, 2025.

[263] W. Zhang, X. Li, G. Shi, X. Chen, Y. Qiao, X. Zhang, X.-M. Wu, and C. Dong, "Real-world image super-resolution as multi-task learning," in *NeurIPS*, vol. 36, 2024.

[264] Y. Poirier-Ginter and J.-F. Lalonde, "Robust unsupervised stylegan image restoration," in *CVPR*, 2023, pp. 22 292–22 301.

[265] L. Xie, C. Zheng, W. Xue, L. Jiang, C. Liu, S. Wu, and H. S. Wong, "Learning degradation-unaware representation with prior-based latent transformations for blind face restoration," in *CVPR*, 2024, pp. 9120–9129.

[266] P. N. Michelini, Y. Lu, and X. Jiang, "edge-SR: super-resolution for the masses," in *WACV*, 2022, pp. 1078–1087.

[267] X. Zhang, H. Zeng, and L. Zhang, "Edge-oriented convolution block for real-time super resolution on mobile devices," in *ACM MM*, 2021, pp. 4034–4043.

[268] B. Xia, Y. Zhang, Y. Wang, Y. Tian, W. Yang, R. Timofte, and L. Van Gool, "Basic binary convolution unit for binarized image restoration network," *ICLR*, 2023.

[269] R. Wei, Z. Liu, Y. Fan, R. Wang, R. Huang, and M. Li, "SCALES: Boost binary neural network for image super-resolution with efficient scalings," in *DATE*, 2025.

[270] T. Song, G. Jin, P. Li, K. Jiang, X. Chen, and J. Jin, "Learning a spiking neural network for efficient image deraining," in *IJCAI*, 2024, pp. 1254–1262.

[271] X. Su, C. Wu, and Z. Zheng, "Bridge the gap between SNN and ANN for image restoration," *arXiv preprint arXiv:2504.01755*, 2025.

[272] Y. Li, K. Zhang, J. Liang, J. Cao, C. Liu, R. Gong, Y. Zhang, H. Tang, Y. Liu, D. Demandolx *et al.*, "LSDIR: A large scale dataset for image restoration," in *CVPR*, 2023, pp. 1775–1787.

[273] H. Wu, Z. Zhang *et al.*, "Q-Instruct: Improving low-level visual abilities for multi-modality foundation models," in *CVPR*, 2024, pp. 25 490–25 500.

[274] X. Jin, Y. Shi, B. Xia, and W. Yang, "LLMRA: Multi-modal large language model based restoration assistant," *arXiv*, 2024.

[275] X. Xu, S. Kong, T. Hu, Z. Liu, and H. Bao, "Boosting image restoration via priors from pre-trained models," in *CVPR*, 2024, pp. 2900–2909.

[276] B. Zheng, J. Gu, S. Li, and C. Dong, "LM4LV: A frozen large language model for low-level vision tasks," *arXiv preprint arXiv:2405.15734*, 2024.

[277] X. Deng and P. L. Dragotti, "Deep convolutional neural network for multi-modal image restoration and fusion," *IEEE Trans. Pattern Anal. Mach. Intell.*, vol. 43, no. 10, pp. 3333–3348, 2020.

[278] Y. Zhang, C. Peng, Q. Wang, D. Song, K. Li, and S. K. Zhou, "Unified multi-modal image synthesis for missing modality imputation," *IEEE Trans. Med. Imaging*, 2024.

[279] Z. Zhao, H. Bai, J. Zhang, Y. Zhang, K. Zhang, S. Xu, D. Chen, R. Timofte, and L. Van Gool, "Equivariant multi-modality image fusion," in *CVPR*, 2024, pp. 25 912–25 921.

[280] J. Ma, Y. Ma, and C. Li, "Infrared and visible image fusion methods and applications: A survey," *Inf. Fus.*, vol. 45, pp. 153–178, 2019.

[281] J. Liang, J. Cao, Y. Fan, K. Zhang, R. Ranjan, Y. Li, R. Timofte, and L. Van Gool, "VRT: A video restoration transformer," *IEEE Trans. Image Process.*, 2024.

[282] K. Zhou, W. Li, Y. Wang, T. Hu, N. Jiang, X. Han, and J. Lu, "NeR-FLix: High-quality neural view synthesis by learning a degradation-driven inter-viewpoint mixer," in *CVPR*, 2023, pp. 12 363–12 374.

[283] D. Li, K. Ma, J. Wang, and G. Li, "Hierarchical prior-based super resolution for point cloud geometry compression," *IEEE Trans. Image Process.*, 2024.

[284] L. Wang, T.-K. Kim, and K.-J. Yoon, "EventSR: From asynchronous events to image reconstruction, restoration, and super-resolution via end-to-end adversarial learning," in *CVPR*, 2020, pp. 8315–8325.

[285] Q. Liang, X. Zheng, K. Huang, Y. Zhang, J. Chen, and Y. Tian, "Event-Diffusion: Event-based image reconstruction and restoration with diffusion models," in *ACM MM*, 2023, pp. 3837–3846.

[286] L. Pang, X. Rui, L. Cui, H. Wang, D. Meng, and X. Cao, "HIR-Diff: Unsupervised hyperspectral image restoration via improved diffusion models," in *CVPR*, 2024, pp. 3005–3014.



Junjun Jiang received the B.S. degree in Mathematics from the Huaqiao University, Quanzhou, China, in 2009, and the Ph.D. degree in Computer Science from the Wuhan University, Wuhan, China, in 2014.

From 2015 to 2018, he was an Associate Professor with the School of Computer Science, China University of Geosciences, Wuhan. From 2016 to 2018, he was a Project Researcher with the National Institute of Informatics (NII), Tokyo, Japan. He is currently a Professor with the School of Computer Science and Technology, Harbin Institute of Technology, Harbin, China. His research interests include image processing and computer vision.



Zengyuan Zuo received the B.E. degree in the Harbin Institute of Technology (HIT), Harbin, China, in 2024. He is currently pursuing the MA.Eng. degree in Faculty of Computing at Harbin Institute of Technology. His research interests include image restoration.



Gang Wu received the B.E. degree in the School of Computer Science and Technology from Soochow University, Jiangsu, China, in 2020. He is currently pursuing the Ph.D. degree in Faculty of Computing at Harbin Institute of Technology. His research interests include image restoration, representation learning, and self-supervised learning.



Kui Jiang received the Ph.D. degree in the school of Computer Science, Wuhan University, Wuhan, China, in 2022. He is currently an associate professor with the school of Computer Science and Technology, Harbin Institute of Technology, Harbin, China. He received the 2022 ACM Wuhan Doctoral Dissertation Award. His research interests include image/video processing and computer vision.



Xianming Liu received the B.S., M.S., and Ph.D. degrees in computer science from the Harbin Institute of Technology (HIT), Harbin, China, in 2006, 2008, and 2012, respectively. In 2011, he spent half a year at the Department of Electrical and Computer Engineering, McMaster University, Canada, as a Visiting Student, where he was a Post-Doctoral Fellow from 2012 to 2013. He was a Project Researcher with the National Institute of Informatics (NII), Tokyo, Japan, from 2014 to 2017. He is currently a Professor with the School of Computer Science and Technology, HIT. His research interests include trustworthy AI, 3D signal processing and biomedical signal processing.